Field Calibration and PAS-SIM Model Evaluation of the XAD-based Passive Air Samplers for Semi-volatile Organic Compounds

Yuening Li,[1] Faqiang Zhan,[1*] Ying Duan Lei,[1] Chubashini Shunthirasingham,[2] Hayley Hung,[2] Frank Wania[1*]

1. *Department of Physical and Environmental Sciences, University of Toronto Scarborough, 1265 Military Trail, Toronto, Ontario, Canada M1C 1A4*

2. *Air Quality Processes Research Section, Environment and Climate Change Canada, 4905 Dufferin Street, Toronto, Ontario, Canada M3H 5T4*

TOC Art

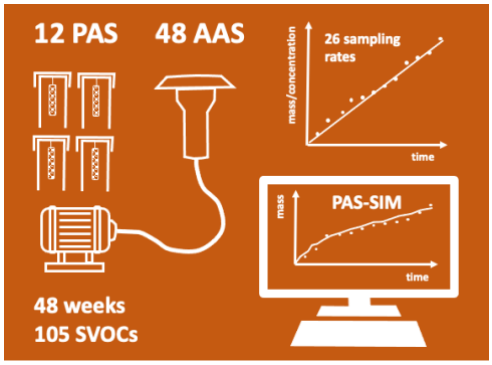

Synopsis

A year-long calibration study confirms that the linear uptake period of a passive air sampler using XAD-resin sorbent is longer than estimated with a simulation model and much longer than those of samplers using polyurethane or polyethylene as sorbents.

Keywords:

SVOCs, XAD-PAS, calibration, sampling rate, linear uptake, model evaluation

Abstract

The use of passive air samplers (PAS) for semi-volatile organic compounds (SVOCs) continues to expand. To advance quantitative understanding of uptake kinetics, we calibrated the XAD-PAS, using a styrene-divinylbenzene sorbent, through a year-long side-by-side deployment with an active sampler. Twelve XAD-PASs, deployed in June 2020, were retrieved at 4-week intervals, while gas phase SVOCs were quantified in 48 consecutive week-long active samples taken from June 2020 to May 2021. Consistent with XAD's high uptake capacity, even relatively volatile SVOCs, such as hexachlorobutadiene, displayed linear uptake throughout the entire deployment. Sampling rates (*SR*s) range between 0.1 and 0.6 $m^3 \cdot day^{-1}$ for 26 SVOCs, including brominated flame retardants, organophosphate esters, and halogenated methoxylated benzenes. *SR*s are compared with experimental *SR*s reported previously. The ability of the existing mechanistic uptake model PAS-SIM to reproduce the observed uptake and *SR*s was evaluated. Agreement between simulated and measured uptake curves was reasonable, but varied with compound volatility and the assumed stagnant air layer boundary thickness. Even though PAS-SIM succeeds in predicting the *SR* range for the studied SVOCs, it fails to capture the volatility dependence of the *SR* by underestimating the length of the linear uptake period and by failing to consider the kinetics of sorption.

1. INTRODUCTION

Semi-volatile organic chemicals (SVOCs) with a vapour pressure between 10^{-6} to 10^{-1} Pa can occur in both the atmospheric gas and particle phases.[1] This group of compounds comprises a large number of legacy and emerging organic contaminants, such as halogenated flame retardants (HFRs), organochlorine pesticides (OCPs), organophosphate esters (OPEs), and neutral per-and polyfluoroalkyl substances (nPFASs). Some SVOCs are classified as persistent organic pollutants (POPs), as they are persistent, have the potential for bioaccumulation and long-range transport (LRT), and can cause adverse effects on human and environmental health. The adverse effects include, but are not limited to, hormone disruption, cardiovascular and metabolic diseases, cancer, and reproductive and neurological problems.[2–4] Even though SVOCs are mainly produced and used in populated areas, LRT can deliver some SVOCs to remote regions.[5,6] The atmosphere is particularly efficient in dispersing SVOCs and facilitating the exposure of organisms to SVOCs.[7] Therefore, it is essential to know the concentration and spatial distribution of SVOCs in the atmosphere, which in turn requires reliable techniques for sampling trace amounts of SVOCs from air.

Air samplers for SVOCs fall into two categories: active air samplers (AAS) and passive air samplers (PAS). AASs rely on a pump to pass air through or over the sampling medium (e.g., a sorbent or a filter), which retains the target chemicals. If the AAS strips the target compounds completely from the air, accurate sampling volumes are easily established. Sometimes, an effort is made to separate the gas and particle phase during sampling. The ability of pumps to strip chemicals from large air volumes allows concentrations in the gas and particle phase to be obtained with high temporal resolution.[8,9] The shortcomings of AASs include high maintenance requirements and operational expenses and the need for a stable electrical power supply. In contrast to AASs, chemical vapours diffuse to a PAS's sorbent over its deployment length. By eliminating the need for a pump, PASs are particularly suited for deployments in areas without reliable electrical power supply. While the slowness of chemical uptake in PASs prevents sampling with a high temporal resolution, a PAS capable of time-integrated sampling over extended periods of time can be advantageous when frequent access to a sampling site is difficult. Because the cost and maintenance requirements for PASs are much lower compared to AASs, the ability to sample simultaneously at multiple sites makes PASs also well-equipped to provide data at high spatial resolution.[9] The main disadvantage of PASs is the challenge to accurately quantify the sampled air volume.

PASs for SVOCs differ in terms of the sorbent used. Whereas some natural sampling media, such as plant foliage, have been used for monitoring atmospheric SVOCs,[10,11] their uptake capacities and kinetics are related to species, location, and growth, which may cause high uncertainties and limit the range of their applications.[12] In contrast, the consistency of artificial sorbents increases data comparability when sampling at different locations or during different periods.[13] Among the man-made sorbents, polyurethane foam (PUF) is widely used in sampling SVOCs from the atmosphere because of its ease of handling and reasonably high and consistent sorptive capacity.[14–19] However, the sorptive capacity of PUF for many more volatile SVOCs is too small to avoid sampling in the curvilinear regime or even reaching equilibrium. This adds hurdles and uncertainties for experimental design and data interpretation during the use of PUF-based PASs.[20,21] Sampling in the linear uptake range is more easily achieved using a sorbent with a higher uptake capacity, such as styrene-divinylbenzene co-polymeric resin (commercial name XAD). Some PASs utilize other sorbents like polyethylene (PE), ethylene-vinyl acetate (EVA), and polydimethylsiloxane (PDMS),[7] but these sorbents, with lower uptake capacity and stability, are less frequently and less widely used than PUF and XAD resin.

XAD is a divinylbenzene styrene copolymer, and the XAD resin is classified into several types (e.g., XAD-2, XAD-4, XAD-16, etc.) based on polarity, pore size, and surface area. XAD resins were first used in the analysis of water samples,[22–24] and XAD-2 was first used for the sampling of organic vapours in 1974.[25] XAD is a granular adsorbent with a high uptake capacity for SVOCs, and many chemicals are more stable on XAD than on PUF over long periods of deployment or storage.[26] Several PASs rely on XAD as a sorbent. Wania et al.[13] introduced a XAD-based passive air sampler (XAD-PAS) comprising a stainless-steel mesh cylinder filled with XAD-2 resin and hung into an inverted cylindrical steel can. Gong et al.[27] modified the housing of this PAS to reduce the effect of wind speed on sampling rates. Okeme et al.[28,29] developed two types of PASs for indoor use relying on XAD-4 filled stainless steel mesh pocket and XAD-4 coated PDMS. Shoeib et al.[30] impregnated PUF disks with ground XAD-4 powder and used a double bowl housing for their PAS.

Confident use of a PAS requires the knowledge of its uptake kinetics in their dependence on meteorological conditions and chemical properties and of the limits of linear uptake of more volatile SVOCs. Such knowledge is gained through calibration studies involving the side-by-side deployment of active and passive air sampling techniques. During the past two decades, eight research papers have reported on outdoor calibrations of the XAD-PAS developed by Wania et al.[13] for some pesticides,[13,31–33] polychlorinated biphenyls (PCBs),[34] polycyclic

aromatic hydrocarbon (PAHs),[34,35] nPFASs,[36] and volatile methyl siloxanes (VMS)[37]. The longest deployment during most of these outdoor calibration experiments was between three months and one year. Deployment locations included places in tropical,[32,36] subtropical,[33] temperate,[13,31,34,35,37] and polar regions[13]. In these earlier calibrations of the XAD-PAS, the number of samples was not large, the active air sampling was episodic, and the number of quantified chemicals was limited. The latter shortcoming, in particular, may have prevented the wider adoption of this PAS.

Therefore, we describe here a calibration study for the XAD-PAS that aimed to improve on previous efforts by (i) conducting the calibration in an urban area, where concentrations of many SVOCs in the air should be sufficiently high to facilitate reliable quantification, (ii) lasting long enough for the PAS to potentially exceed the linear uptake period of more volatile SVOCs, (iii) including a large number of PAS deployment periods, (iv) involving continuous, rather than episodic, active air sampling using flow rates (mid-volume) and sampling times (1 week) that seek a balance between minimizing break-through losses and collecting sufficient amounts for reliable quantification, and (v) aiming for quantification of a large number of SVOCs, including those without earlier, empirically determined sampling rates. In addition to reporting the results of the calibration, we also use them to evaluate the performance of the PAS-SIM model, which simulates the transport of chemicals from the atmospheric gas phase to the sorbent of a PUF- or XAD-based PAS using a user-friendly Microsoft Excel-based interface.[34]

2. MATERIALS AND METHODS

Field Sampling. 24 short mesh cylinders, filled with precleaned XAD-2 resin (Supelco, Inc, U.S.) (Panel A of Figure 1) were deployed in 12 XAD-PAS housings at a height of ca. 1 m above the ground on a fence on the campus of the University of Toronto Scarborough in the Eastern suburbs of Toronto (43.78371, -79.19027) (Panel B of Figure 1) on June 17, 2020. Every four weeks, the two cylinders from the same XAD-PAS housing were retrieved, with the last pair taken on May 19, 2021 (Panel C of Figure 1). During the entire passive air sampling periods, 48 consecutive week-long active samples were taken with a mid-volume pump (MV-AAS, ~50 L min^{-1}, ~500 m^3 $sample^{-1}$) (Figure 1). For each active sample, the air flow was first passed through a glass fiber filter (GFF) and then a glass cartridge containing XAD-2 resin (15-20 g) placed between two layers of cleaned polyurethane foam (PUF) (Supelco, U.S.). While there is the possibility of filter artifacts during this type of AAS, namely blow-off and

filter adsorption,[38] we consider SVOCs quantified in the extracts of the glass cartridge and GFF to be nominally in the gas and particle phase, respectively.

Six field blanks for PASs and four field blanks for AAS were collected. The XAD-PAS field blanks were samplers that were placed in storage containers in the vicinity of the sampling site on June 17, 2020; one was retrieved at the deployment day,while the others were retrieved after 4, 8, 16, 24 and 48 weeks, respectively. Upon retrieval, mesh cylinders were stored in airtight metal tubes, and cartridges and GFFs were wrapped up in baked aluminum foil and stored in solvent-rinsed glass jars. All samples were stored in a freezer at -20 ℃ prior to extraction. One set of duplicate PAS and the GFFs from the AAS were archived, i.e., we report here the results for one PAS for each deployment period and the gas phase AAS. This implies that we cannot report explicitly on the precision of the amount of a chemical in a XAD-PAS deployed for a particular length of time. However, we do not rely on samplers retrieved at individual time points to derive sampling rates but on a linear regression through all time points. A retrieval strategy that prioritised the number of deployment lengths over replication was believed to strengthen the linear regression analysis. Furthermore, the error of the regression slope provides an indirect estimate of the precision of sampling, extraction and quantification. We also note that replicate precision of XAD-PAS deployments and analyses has been studied numerous times before.[33,39]

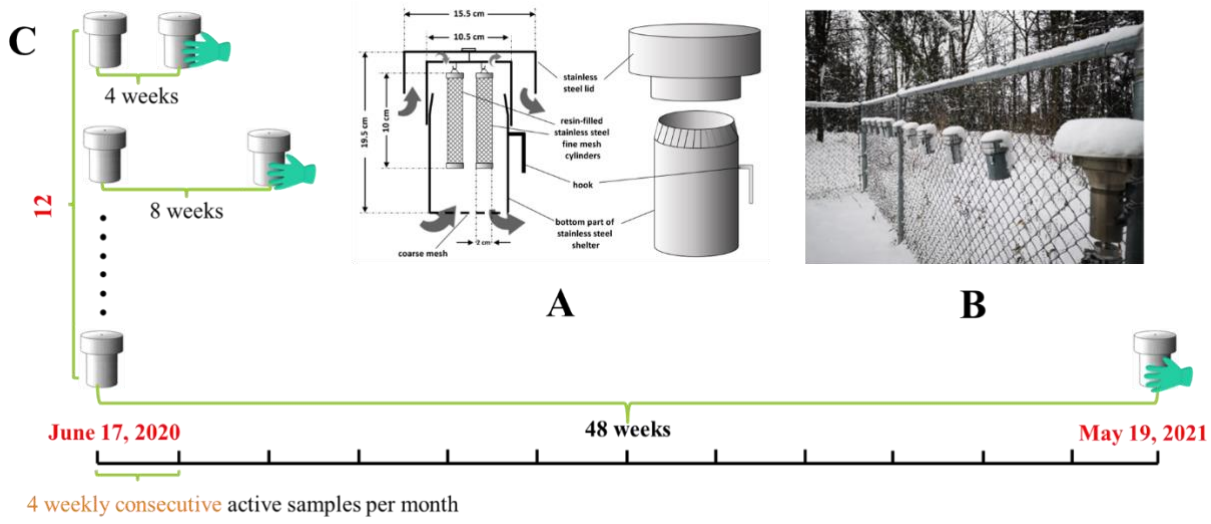

Figure 1. Information on the sampler and the deployment strategy adopted in this calibration study: (A) schematic representation of the short version of the XAD-based passive air sampler; (B) photograph of the sampling site in Toronto, Ontario; (C) schematic diagram of the sampling strategy.

Sample Treatment. Prior to extraction, labeled standards, including, OCPs, HFRs, OPEs, and nPFASs, were spiked onto the samples as surrogates. The samples, i.e., the XAD-2 resin from a XAD-PAS mesh cylinder, and the XAD-2 resin and PUFs from the glass cartridge used in the AAS, were extracted with a 1:1 (v/v) mixture of hexane and acetone using Accelerated Solvent Extraction (ASE 350, Dionex, Sunnyvale, CA, U.S.). Extracts were concentrated using a rotary evaporator, and then went through sodium sulfate (Na_2SO_4) columns to remove water. Extracts were concentrated to ~1 mL using gentle stream of nitrogen and solvent-exchanged into iso-octane with the final volume adjusted to 0.1 mL for PAS extracts and 0.5 mL for AAS extracts. Prior to instrumental analysis, 2−4 ng and 10−20 ng injection standards were added to PAS and AAS extracts, respectively. Details about ^{13}C labeled and deuterated standards and other chemicals are given in Table S1 in the Supporting Information. Here we do not report on the analysis of SVOCs nominally in the particle phase, i.e., sorbed to the GFFs from the AAS.

Instrumental Analysis. The extracts were analysed for the presence of 24 organochlorine pesticides, 5 halogenated methoxy benzenes, 9 other chlorinated compounds, including hexachlorobutadiene, and penta- and hexachlorobenzene, 32 halogenated flame retardants, 16 organophosphate esters, and 14 neutral poly- and perflourinated substances. The complete list of 100 targeted substances is provided in Table S1 in the SI. nPFAS were analyzed by GC-MS operated in selected ion monitoring (SIM) mode under positive chemical ionization (PCI). All other substances were analyzed by GC-MS/MS using electron ionization (EI) in multiple reaction monitoring (MRM) mode. Details on the instruments, GC columns, temperatures and other parameters are given in the Supporting Information (SI).

Ambient Information. Ambient temperature during the sampling period was recorded with an hourly resolution using ibuttons (ibuttonlink, U.S.). Hourly information on wind speed and direction was obtained from the weather station located on the top of the Science Wing Building on the campus of the University of Toronto Scarborough, which is within 200 meters of the sampling site. The meteorological data are shown in Figures S1 & S2 in the Supporting Information.

Quality Assurance and Quality Control. All glassware was machine-washed with detergents and baked at 450 °C in a muffle furnace for over 8 hours to remove potential contaminants. All the other experimental materials coming in contact with the samples or extracts were cleaned and rinsed with solvents three times prior to use. All extraction and concentration procedures were conducted in a trace analytical lab. Seven procedure blanks, which were extracted and analyzed with field blanks and field samples, contained no contaminants above detection limits.

Only a few analytes were detected in the field blanks, and for those analytes, the amounts of target chemicals in PAS and AAS extracts (M_{PAS} and M_{AAS}, ng) were reduced by the average of the amount detected in field blanks. Quantification was done using an internal standard method relying on the spiked labeled chemicals. Therefore, the reported amounts have been corrected for recovery. The recoveries of surrogates are given in Table S2. The method detection limits (MDLs), provided in Table S3, were calculated as three times the standard deviations of the levels in field blanks if the analytes were detected in blanks (the signal-to-noise ratio (S/N) > 3), otherwise they were calculated as the concentrations at which the S/N is 10.

Calculation of Sampling Rates (*SR*). Weekly volumetric air concentrations of SVOCs nominally in the gas phase ($C_{AAS\text{-}W}$, ng m^{-3}) were obtained by dividing M_{AAS} by the corresponding active air sampling volumes. The atmospheric concentration of a chemical over the deployment period of a XAD-PAS (C_{air}, ng m^{-3}) was derived by averaging the weekly $C_{AAS\text{-}W}$ data during this passive air sampling period. Finally, during the linear uptake phase, the *SR* of a chemical was estimated from the slope of a linear regression of this chemical's effective sampling volume (i.e., M_{PAS}/C_{air}) against its deployment length *t* (Eq.1).

$$\frac{M_{PAS}}{C_{air}} = SR \cdot t \quad (1)$$

PAS-SIM Calculations. Experimentally derived uptake curves (i.e., M_{PAS} as a function of *t*) and sampling rates were compared with results obtained with the PAS-SIM model. By simulating the transfer of chemical from the atmosphere across an air-side boundary layer and within the PAS's porous sorbent, this model yields estimated uptake curves and *SR*s.[34] Input parameters for those simulations were the measured gas phase concentrations, $C_{AAS\text{-}W}$, the meteorological data (atmospheric pressure; daily temperature, °C; and hourly wind speed, m s^{-1}), and chemical properties including molecular weight and volume, the partitioning ratio between XAD and air at 20 °C in units of m^3 air m^{-3} XAD ($K'_{XAD/air}$), and the internal energy of phase change between XAD and the gas phase ($\Delta U_{XAD/air}$, J mol^{-1}). The partitioning ratio between XAD and air at 20 °C in units of L air g^{-1} XAD ($K_{XAD/air}$) and $\Delta U_{XAD/air}$ (Table S3) were obtained using poly-parameter linear free energy relationships (ppLFERs)[40] and solute descriptors from the UFZ-LSER database[41]. $K'_{XAD/air}$ was obtained from $K_{XAD/air}$ using the density of the resin (640 kg m^{-3}).[40] The degradation rate of SVOCs sorbed to XAD and the atmospheric aerosol concentration were set to zero. Four values for the thickness of a stagnant air boundary layer surrounding the XAD-resin Δz were used (0.0075, 0.010, 0.015, and 0.020

m).[31,34]

3. RESULTS AND DISCUSSION

Effective Sampling Volumes and Linearity of Uptake. Of the 100 targeted compounds, 45 could be detected consistently (i.e., had detection frequency > 90%) in the extracts of the AAS. Plots of the effective sampling volume (i.e., M_{PAS}/C_{air}) (Table S4) against deployment length were created for 26 chemicals. Examples of such linearized uptake curves for α-1,2-dibromo-4-(1,2-dibromoethyl)cyclohexane (α-TBECH), α-hexachlorocyclohexane (α-HCH), 10:2 fluorotelomer alcohol (10:2 FTOH), and Tris(2-chloroethyl) phosphate (TCEP) are shown in Figure 2; the remaining ones are provided in Figure S3 in the SI. Such plots could not be made for all of the compounds detected in the AAS extracts, because 15 of them could not be reliably quantified in the PAS extracts. Examples of such chemicals are tris (2-butoxyethyl) phosphate (TBEP), 2-ethylhexyl-diphenyl phosphate (EHDPP), and 2,4,4'- tribrominated diphenyl ether (BDE 28). Even at the longest deployment length (48 weeks), the air sampling volumes collected by the XAD-PAS (~130 m^3) is smaller than that collected by an AAS during one week (~500 m^3), which means that compounds with low air concentrations cannot be detected in the PAS if the limit of detection is relatively high.

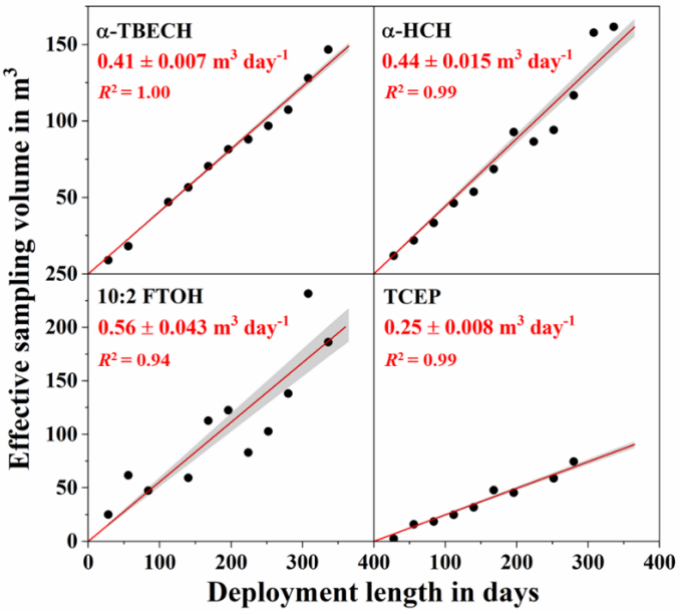

Figure 2: The increase of the effective sampling volume of four representative chemicals throughout the 48-week deployment period. The black markers indicate the field blank-corrected measured values, and the red lines indicate linear regressions forced through the origin. Sampling rates in m^3 day^{-1} are obtained from the slope of these regressions. The shaded areas represent the uncertainties of the calculated sampling rates obtained from the uncertainties of the slopes of these regressions.

For most of the 26 compounds, which could be detected reliably in AAS and PAS extracts, the effective sampling volume had a good linear relationship with deployment length, with R^2 values generally higher than 0.95 (Table 1) and p values lower than 0.05. In particular, for none of the analytes is there any indication of a deviation from linearity towards the end of the 48 weeks of the calibration study. Such deviation would be apparent in a concave tendency toward the end of the deployment period. Even compounds as volatile as hexachlorobutadiene and pentachlorobenzene, which have estimated log ($K_{XAD/air}$/(L air g^{-1} XAD)) values of 2.95 and 3.87 at 20 °C and liquid-state saturation vapour pressures of 29.3 Pa and 1.1 Pa at 25 °C, respectively, show no such trend. Krogseth et al.[37] had previously observed linear uptake in the XAD-PAS for D4 (log ($K_{XAD/air}$/(L air g^{-1} XAD)) = 2.82 at 20 °C, 140 Pa at 25 °C) over a three month calibration period. By contrast, the uptake of SVOCs with vapour pressures as high as 40 Pa at 25 °C has been shown to deviate from linearity in the PUF-PAS after as little as 2 weeks.[42] Similarly, PASs based on PE as a sorbent have been shown to display non-linear uptake for compounds with vapour pressures as high as 0.0023 Pa after a mere 2 weeks.[43]

Using HCB for illustration, Wania and Shunthirasingham[7] recently estimated that the XAD-PAS has a theoretical uptake capacity that is considerably larger than that of most other PASs for SVOCs. This much higher uptake capacity, in combination with slightly lower sampling rates, means that the XAD-PAS operates in the linear uptake regime for much longer and for much more volatile SVOCs than PAS using PUF and PE as a sorbent. While methods have been developed to interprete PAS results obtained in the curvi-linear uptake phase,[12,44–46] the requirement to use often labelled depuration compounds makes these methods expensive and unsuited for indoor deployments. They also incur large uncertainties[20] and rely on assumptions, e.g. related to the constancy of air concentrations over time, that are often not valid.[7] The linearity of the uptake in the XAD-PAS observed here thus confirms theoretical expectations and justifies its use without the use of depuration compounds. Only the sampling rates needs to be known for a quantitative interpretation of results obtained with the XAD-PAS during deployment periods up to one year as long as the targeted compounds have a log ($K_{XAD/air}$/(L air g^{-1} XAD)) above 3 at 20 °C or a vapour pressure at 25 °C below 30 Pa.

Sampling Rates. Sampling rates (*SR*s) for 26 compounds in units of m^3 day^{-1}, estimated from the slopes of the linear regressions (Figure 2, Figure S3), are listed in Table 1, together with the uncertainty estimated from the standard error of the slope of the linear regression, which is on the order of 1.7 to 10.5 %. These are the first ever reported *SR*s for three brominated flame retardants, six organophosphate esters, and four halogenated methoxylated benzenes (Table 1).

Also, *SR*s for HCBD, pp'-DDE and PeCB have not previously been reported. The *SR*s determined in this study range between 0.1 and 0.6 m^3 day^{-1}. Even though the $K_{XAD/air}$ at 20 °C of the 26 compounds in Table 1 varies over six orders of magnitude, the range of the sampling rates is within a factor of 6. There is tendency for the *SR* to increase with the volatility of the compound (Figure 3). The *SR*s of OPE tend to be lower than those of halogenated compounds with the same adsorption coefficient to XAD-resin.

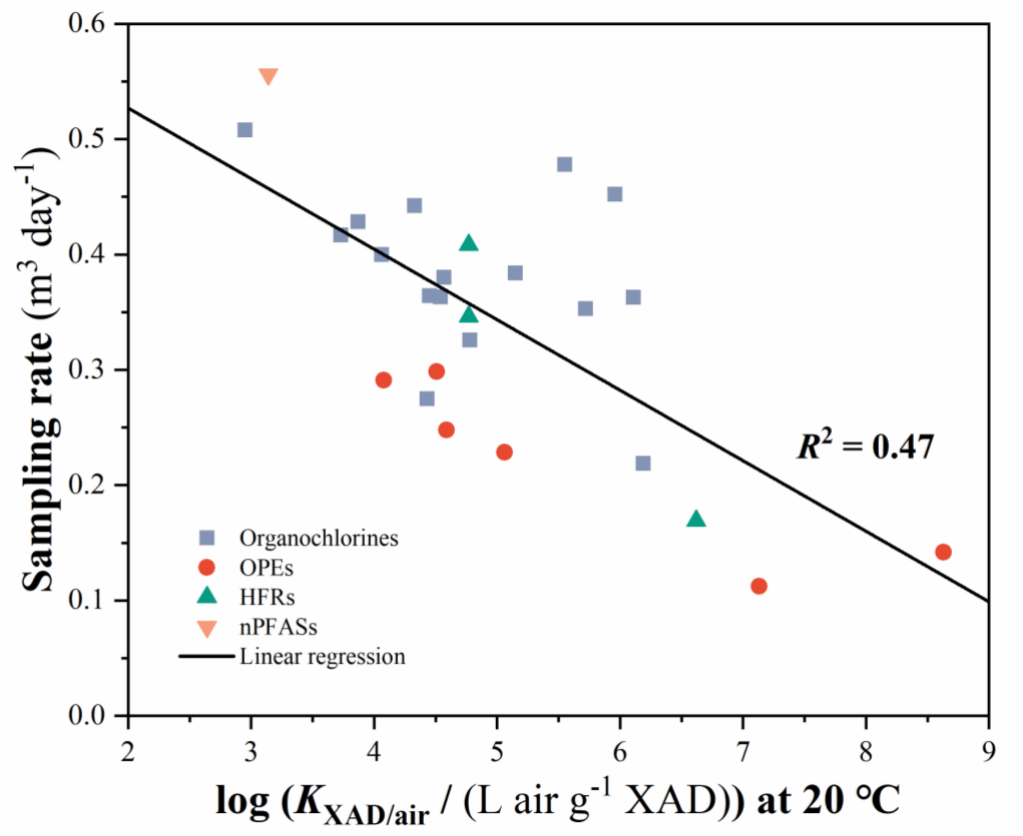

Figure 3: The increase of the sampling rates of 26 chemicals with an increase in volatility. The markers in different colors indicate sampling rates of different chemical groups, and the black line indicates a linear regression between sampling rate and log $K_{XAD/air}$ at 20 °C.

Comparison with previously reported *SR*s. Previously reported *SR*s for HCB and six organochlorine pesticides in the XAD-PAS are included in Table 1 for comparison. *SR*s derived from earlier calibrations relying on the long version of the XAD-PAS (20 cm long mesh cylinders) were divided by two, because the *SR* is proportional to the surface area of the resin that is exposed to the atmosphere.[47] The *SR* for *cis*- and *trans*-chlordane and *trans*-nonachlor (CC, TC, and TN) reported here are highly consistent with those reported previously.[13,31–33] In the case of compounds for which the range of previously reported *SR*s is quite large (α- and γ-HCH, HCB, dieldrin, 2-(perfluorodecyl) ethanol (10:2 FTOH),[13,31–33] our *SR*s are at the lower end of the reported range.

Table 1 Passive Sampling Rates (m^3 d^{-1}) Determined for the Target Chemicals in Our Study and Reported in Literature (Conducted at Locations with Different Climates)

Chemicals[1]	log ($K_{XAD/air}$ / L air g^{-1} XAD) at 20 °C[2]	Experimentally determined		
		***SR* in our study[3]**	***R*²**	***SR* in literature**
Halogenated methoxybenzene				
TBA	3.73	0.42 ± 0.018	0.98	
TeCV	4.43	0.27 ± 0.010	0.99	
DAME	4.78	0.33 ± 0.012	0.99	
PCA	4.54	0.36 ± 0.014	0.98	
Industrial organochlorines				
HCBD	2.95	0.51 ± 0.021	0.98	
PeCB	3.87	0.43 ± 0.017	0.98	
HCB	4.06	0.40 ± 0.017	0.98	0.30 *[13], 0.56 *[13], 0.84 *[13], 0.86 [31], 2.0 *[32], 1.36 [33]
Organochlorine pesticides				
α-HCH	4.33	0.44 ± 0.015	0.99	0.21 *[13], 0.63 *[13], 1.23 *[13], 1.06 [31], 1.58 [33]
γ-HCH	4.45	0.36 ± 0.013	0.99	0.32 *[13], 0.75 *[13], 0.91 [31], 1.51 [33]
δ-HCH	4.57	0.38 ± 0.029	0.96	
Heptachlor	5.72	0.35 ± 0.018	0.97	
TC	5.15	0.38 ± 0.021	0.97	0.55 [31], 0.55 *[32], 0.46 [33]
CC	5.55	0.48 ± 0.020	0.98	0.43 [31], 0.45 *[32], 0.46 [33]
TN	5.96	0.45 ± 0.014	0.99	0.29 *[13], 0.41 [31], 0.40 *[32], 0.64 [33]
Dieldrin	6.19	0.22 ± 0.022	0.92	0.20 *[13], 1.45 *[32]
pp'-DDE	6.11	0.36 ± 0.032	0.95	
Organophosphate esters				
TPrP	4.08	0.29 ± 0.019	0.96	
TBP	5.06	0.23 ± 0.013	0.97	
TCEP	4.59	0.25 ± 0.008	0.99	
TCPP	4.51	0.30 ± 0.023	0.95	
TPhP	7.13	0.11 ± 0.012	0.91	
TEHP	8.63	0.14 ± 0.015	0.93	
Halogenated flame retardants				
α-TBECH	4.77	0.41 ± 0.007	1.00	
β-TBECH	4.77	0.35 ± 0.012	0.99	
BDE-47	6.62	0.17 ± 0.015	0.92	
Neutral perfluoroalkyl substances				
10:2 FTOH	3.14	0.56 ± 0.043	0.94	0.78 *[36], 2.32 *[36]

[1] The full names of these chemicals are given in Table S3 in SI.

[2] The partitioning ratios between XAD and air at 20 °C ($K_{XAD/air}$, L air g^{-1} XAD) were calculated based on poly-parameter free energy relationships (ppLFERs) in the UFZ-LSER data base[41] and converted using the density of XAD-2 resin (640 kg m^{-3})[40].

[3] The uncertainties were estimated from the standard errors of the slopes of the linear regressions.

* The originally reported sampling rates are for the long version XAD-PAS, i.e., the length of XAD-2 mesh cylinders is 20 cm; thus, in this table, they were converted to the sampling rates of short version XAD-PAS (10 cm length) by dividing by 2.

Some level of variability in *SR*s between different calibration studies is expected, e.g., because

wind can be expected to have some influence on the kinetics of uptake, especially at higher wind speeds.[34,48] Furthermore, the diffusivity of a chemical in the air is positively related to ambient temperature.[49] Higher temperatures at tropical[32] and subtropical[33] locations can accelerate the diffusivity of SVOCs in the gas phase relative to locations in temperate[13,31] and arctic regions[15], which may be partly responsible for variability in the reported *SR*s. Higher *SR* are indeed generally observed during calibrations conducted at warmer locations. However, the observed influence of temperature on *SR* appears larger than what can be explained by the temperature dependence of gas phase diffusivity.

Uncertainties in the average air concentration during the calibration period could be another source of discrepancy in *SR*s between different studies. In the first calibrations study,[13] no AAS-derived concentrations from the period of PAS deployment was available, but they had to be extrapolated from earlier measurements. Also, the AAS measurements in that early study[13] relied only on PUF to collect the gas phase compounds, which is a method susceptible to break-through losses of more volatile analytes.[50,51] In other cases, the AAS operated only during a small fraction of the total PAS deloyment period, and it was assumed that the concentration during that time was representative of the entirety of the calibration period. According to equation 1, if C_{air} is too low, the estimated *SR*s would be too high. Previously published *SR*s that are generally higher than what we report here could therefore be due to earlier studies failing to (1) account for break-through losses of the more volatile analytes during active sampling, or (2) sample episodes of elevated C_{air} with the AAS. In particular, we suspect that the relatively high *SR*s reported for HCB and the HCHs in Wania et al.[13] are biased high because of break-through losses of the AAS technique at the two southern sampling locations.[51] We note that this early study[13] reported lower sampling rates in better agreement with what we report here when the potential for break-through is small, i.e., for (i) HCB and HCHs at the Arctic site of Alert, which has much lower temperatures, and (ii) dieldrin and trans-nonachlor, which are much less volatile.

Going forward, we recommend the use of the lower *SR*s for OCPs reported here, because the use of continuous AAS with a sorbent not susceptible to break-through and the large number of PAS deployments should make them more reliable than those derived from earlier efforts. We note that the range of *SR* for 26 very diverse chemicals is smaller than the ranges in *SR* for OCPs that have been reported previously.[13,31–33]

PAS-SIM Model Evaluation. The uptake curves of the chemicals in Table 1, as simulated using PAS-SIM, are compared with the measured uptake in the bottom panels of Figures 4 and

5 and Figures S4 and S5 in the SI. The temporal variability of the air concentrations during the calibration period is shown with red markers in the upper panels of those figures. Because the sampling period started in early summer and ended in spring, and because the concentrations of most of the investigated SVOCs has a summer maximum and a winter minimum, the air concentrations were generally high during the first third of the calibration period and low during the remainder. Accordingly, the uptake curves generally show a steep increase in the sequestered amounts initially and a generally slower increase later on. Incidentally, this is why a linearization procedure, as applied during the calculation of effective sampling volumes in Figure 2, is required for the derivation of *SR*s.

To illustrate the uncertainty in the calculated uptake, four curves with different assumptions regarding the thickness of the stagnant boundary layer surrounding the sampling sorbent (Δz) are displayed. For the majority of compounds (19 out of 26), a reasonable agreement between simulated and measured uptake is apparent, i.e., the shapes of the uptake curves are generally similar, and the magnitude of uptake is within the range of predicted uptake. There is some variability in the extent of model-measurement agreement within this group, with some compounds showing good matches in the shape of the uptake curve, e.g., the three HCH isomer, the three chlorinated methoxybenzenes (TeCV, DAME, PCA), the chlordane related compounds (TC, CC, TN) and the two TBECH isomers. For other compounds (e.g., pp'-DDE, TPrP, and TCPP), the level of agreement is less impressive, i.e., while the magnitude of uptake is similar in measurement and model, the shape of the uptake is less congruent (Figure S4). In some instances (e.g., pp'-DDE), this could be related to uncertainties in the measured concentrations at levels close to the detection limit.

Theoretically, one would expect a single value of the boundary layer thickness Δz to apply to all chemicals during the same deployment period. However, for different compounds the best model-measurement match is achieved with different values of Δz. For example, for α-HCH, HCB, TC, TN, and α-TBECH, good agreement is attained when Δz is 0.01 m, whereas for DAME, PCA, Heptachlor, and β-TBECH a value of Δz of 0.015 m gives a better fit. Similarly, using a Δz of 0.02 m best simulates the uptake for TeCV, TBP and TCEP. For three chemicals, (TPhP, TEHP, BDE-47), the PAS-SIM model clearly overpredicted uptake (Figure 5, top row). While the shape of the uptake curve is reasonably captured, Δz values exceeding the explored range from 0.0075 to 0.02 m would be required to reproduce the amounts taken up.

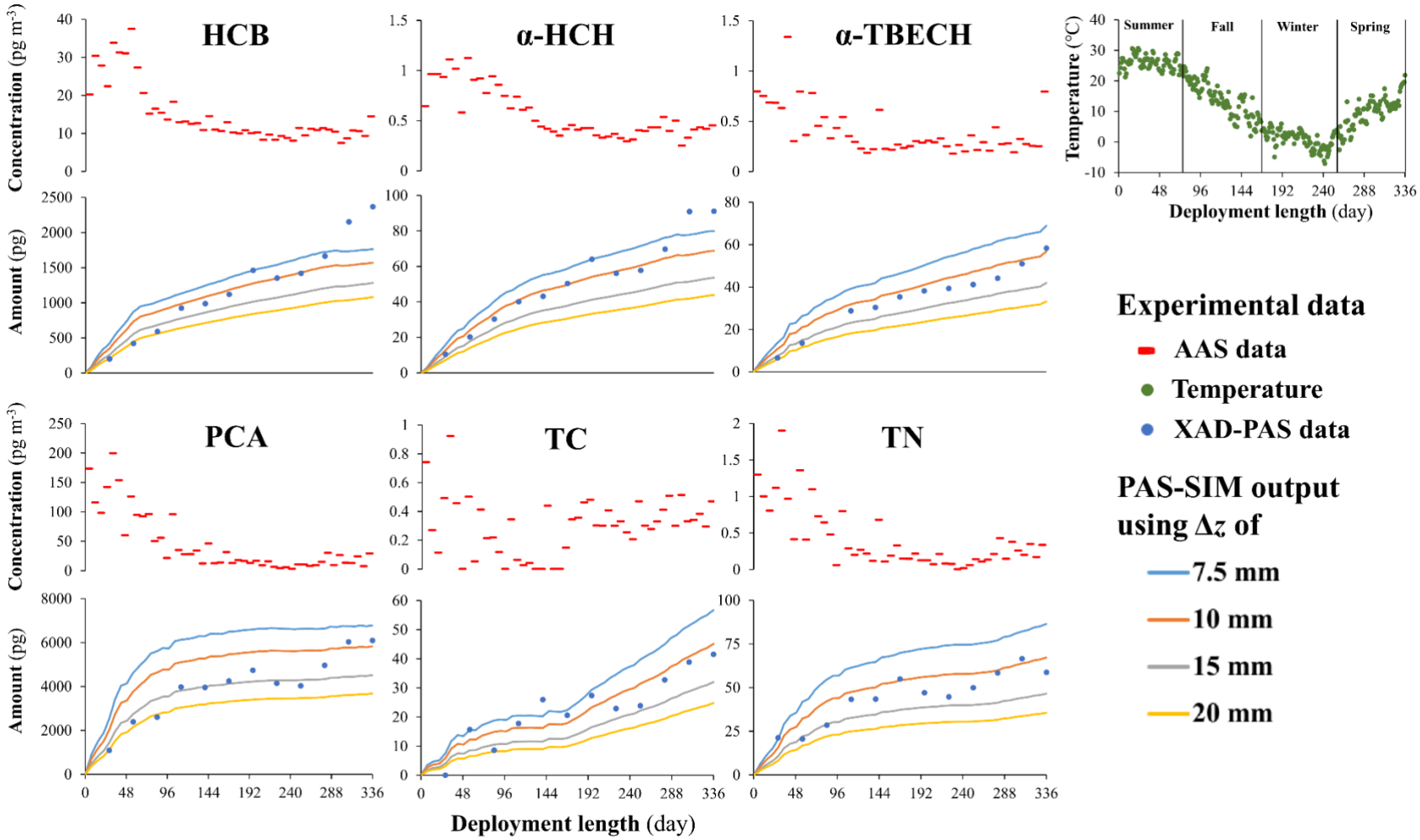

Figure 4: PAS-SIM results for six representative chemicals showing good agreement with measured uptake curves. The red lines in the upper portion of each panel display air concentrations (pg m^{-3}) measured by active air sampling, the blue, orange, prey, and yellow lines are the PAS-SIM model outputs (pg per sampler) under different assumptions regarding the thickness of the stagnant air boundary layer *Δz* of 7.5, 10, 15, and 20 mm , and the dark blue dots are the experimental data of XAD-PAS obtained from the calibration study (pg per sample). Green markers in the upper right panel display ambient temperature (°C).

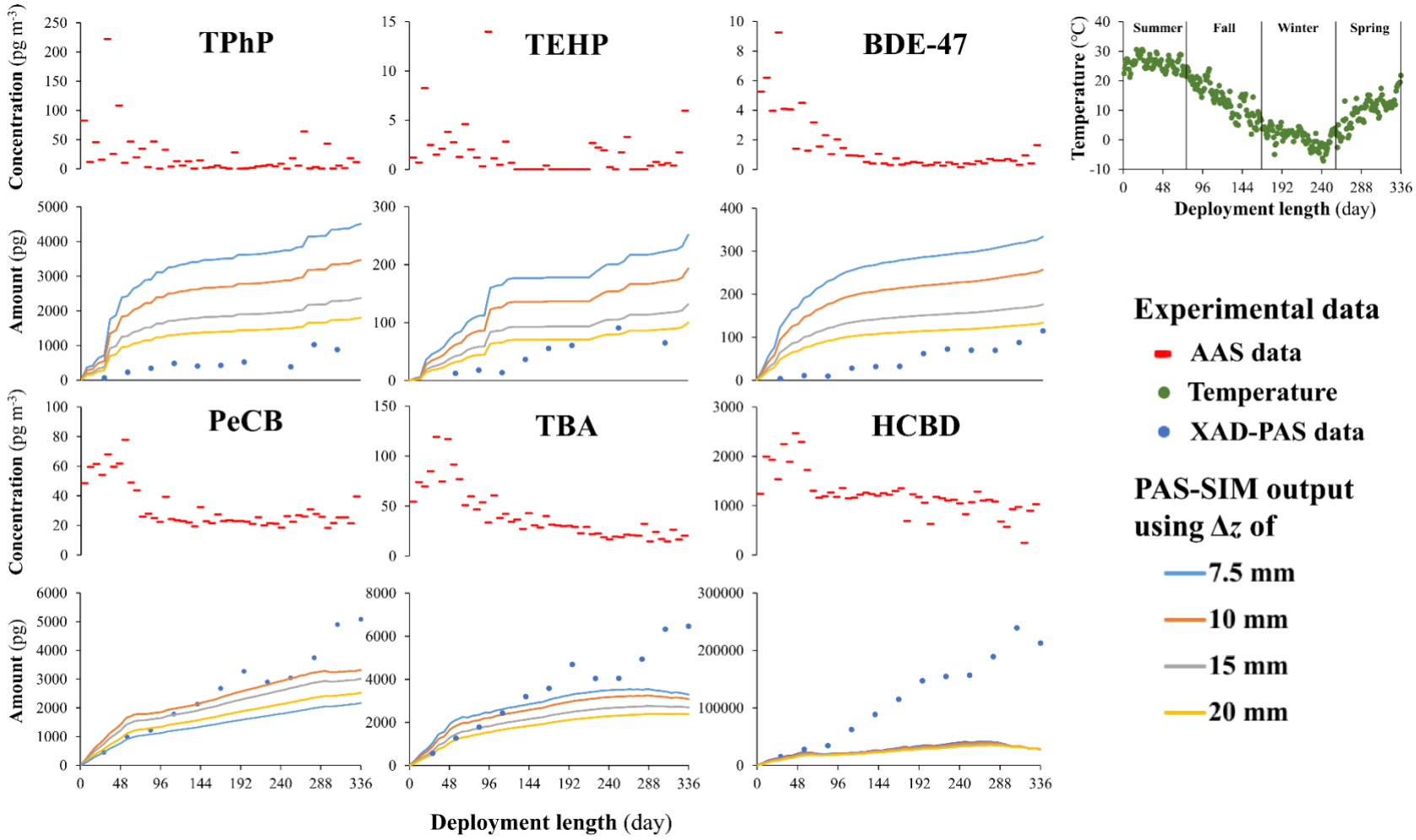

374

375 **Figure 5:** PAS-SIM simulation results for chemicals showing either consistent overprediction (top row) or consistent underprediction (bottom row) relative to
376 the measured uptake curves. The red lines in the upper portion of each panel display air concentrations (pg m^{-3}) measured by active air sampling,
377 the blue, orange, prey, and yellow lines are the PAS-SIM model outputs (pg per sampler) under different assumptions regarding the thickness of the
378 stagnant air boundary layer Δz of 7.5, 10, 15, and 20 mm, and the dark blue dots are the experimental data of XAD-PAS obtained from the calibration
379 study (pg per sample). Green markers in the upper right panel display ambient temperature (°C),

A source of model-measurement discrepancy may be uncertainties in the $K_{XAD/air}$ and $\Delta U_{XAD/air}$ used in the PAS-SIM simulations. Except for HCB, $K_{XAD/air}$ for the chemicals studied here have not been measured and therefore had to be predicted. The ppLFER-predicted and measured $K_{XAD/air}$ values (extrapolated from measurements at higher temperatures) for HCB show some discrepancy.[40] Due to the lack of experimental solute descriptors, the $K_{XAD/air}$ and $\Delta U_{XAD/air}$ of some compounds (e.g., TEHP) had to be calculated using solute descriptors estimated with quantitative structure property relationships, which incur relatively larger uncertainties.[41]

For four compounds (PeCB, TBA, HCBD, 10:2 FTOH), the PAS-SIM model underestimated uptake in the XAD-PAS (Figure 5 bottom row, Figure S5). This overestimation is relatively small for PeCB and TBA, but very pronounced for HCBD and 10:2 FTOH. These four compounds are all relatively volatile (log ($K_{XAD/air}$/(L air g^{-1} XAD)) < 4.0), especially HCBD and 10:2 FTOH. The PAS-SIM model predicts that these chemicals have entered the curvilinear uptake regime (PeCB and TBA) or even reached equilibrium (HCBD and 10:2 FTOH). Our measurements demonstrate that this is not the case and even volatile SVOCs, such as HCBD, maintain linear uptake throughout the entire 48-week field deployment. It suggests that PAS-SIM underestimates the extent to which such SVOCs are diffusing into the inside of the sorbent cylinder. Previously, Armitage et al.[34] and Ramirez-Restrepo et al.[31] have similarly indicated a tendency of PAS-SIM to underpredict the uptake observed for the more volatile OCPs and PAHs. While poor model performance is not desirable, it is of course good that the empirical data suggest that the XAD-PAS displays linear uptake behaviour for relatively more volatile compounds and for longer deployment periods than what PAS-SIM predicts.

Sampling Rate Estimation and Model Performance. We also estimated *SR*s from the PAS-SIM modelling results, using the slope of a linear regression between the predicted effective sampling volumes and deployment time. The *SR*s for the 26 chemicals in Table 1, calculated using four different values of Δz, are given in Table S5. The averages of the estimated *SR*s for 22 chemicals (all in Table 1, except those for which PAS-SIM incorrectly predicted non-linear uptake) ranges from 0.25 m^3 day^{-1} when applying a Δz of 0.020 m to 0.53 m^3 day^{-1} for a Δz of 0.0075 m. Using Δz of 0.015 m yields an average *SR*s (0.31 ± 0.04 m^3 day^{-1}) that is close to the average of the measured *SR* for the same set of chemicals (0.32 ± 0.10 m^3 day^{-1}).

The estimated *SR* increases with a chemical's log $K_{XAD/air}$ at 20 °C, whereby the relative increase is larger when Δz is small and almost non-existent with a Δz of 0.02 m (Figure S6). In other words, PAS-SIM predicts higher sampling rates for less volatile chemicals. This is a result of

PAS-SIM predicting small deviations from linear uptake during the 48 weeks of deployment, whereby this deviation increases with the volatility of a compound. Our measured *SR*s display the opposite behaviour, i.e., we find a tendency towards higher *SR*s for the more volatile compounds (Figure 3). This is yet another indication that the XAD-PAS has a longer linear uptake than PAS-SIM predicts.

The PAS-SIM model does not include a parameterisation of the kinetics of sorption to the sorbent. Therefore, it can only predict *SR*s that increase with volatility, if uptake remains in the linear uptake range and is limited by the diffusion through the air boundary layer. This is because more volatile chemicals tend to be smaller and therefore diffuse slightly faster than larger, less volatile ones. However, this would only result in a very small variability in *SR*, because the molecular gas phase diffusivity of SVOC varies over a very small range. The more complex model of uptake in a PAS by Zhang and Wania[52] does account for the kinetics of sorption and indicates that the *SR* is predicted to increase with compound volatility if a sampler is characterised by relatively slow sorption kinetics and high $K_{XAD/air}$.[52] For the compounds in Table 1, with log ($K_{XAD/air}$/(L air g^{-1} XAD)) between 3 and 7, the rate of sorption k_{sorb} would need to be less than ~10^6 day^{-1} for the *SR* to increase with compound volatility. We conclude that while PAS-SIM succeeds in predicting the range of the *SR* for the SVOCs studied here, it fails to capture the volatility dependence of the *SR*, because it cannot describe the kinetics of sorption and underestimates the length of the linear uptake period.

Importance and Implications. The XAD-PAS has several desirable attributes: The very high uptake capacity of its sorbent allows for sampling in the linear uptake range even for relatively volatile SVOCs over extended deployment periods, greatly simplifying quantitative interpretation, and thereby reducing the uncertainty associated with the calculation of volumetric concentrations in samplers with lower capacity.[20] By preventing wind from blowing onto the sorbent, the housing design of the XAD-PAS avoids the sampling of particle-bound SVOCs[34,53,54] and greatly reduces the wind speed dependence of the *SR*.[48] This reduces the uncertainty associated with widely varying particle sampling rates[42,55] and yields clearly defined gas phase concentrations. If average wind speed during deployment is available, *SR*s can be adjusted using an empirical wind speed correction equation.[48] At wind-exposed sampling sites, a wind-buffered housing can further reduce the effect of wind.[27] Furthermore, a thorough mechanistic understanding of uptake in the sampler exists.[47,52,56,57] What may so far have stood in the way of a wider adoption of the XAD-PAS is possibly a lack of a wider appreciation of these advantages as well as a dearth of empirically determined *SR*s for a larger

variety of SVOCs.

This study sought to address this knowledge gap by performing a calibration study that not only includes a wide range of potential target substances, but also adheres to high expectations with respect to how a passive sampler for SVOCs should be calibrated. This comprises (i) an overall calibration period, that is sufficiently long to test for the linearity of uptake for a wide range of compound volatilities; (ii) a large number of passive sampler deployment periods to obtain a sufficient number of samples for reliable sampling rate derivation; (iii) continuous, instead of episodic, active air sampling with a method not susceptible to break-through loss during the entire calibration period to assure that true time-averaged air concentrations are used for calibration. Many PAS calibration studies do not fulfill even one of these three criteria, and to the best of our knowledge this is the first calibration of a PAS for SVOCs that meets all three. This study confirmed the linear sampling of even volatile SVOCs in the XAD-PAS for deployment of at least 48 weeks. Whereas some earlier studies using the XAD-PAS had to rely on estimated or generic *SR*s,[58] the data presented in this study will allow for the confident application to a wider range of SVOCs using compound-specific *SR*s.

Considering the variability of *SR* with log $K_{XAD/air}$ that we observed, it is reasonable to expect that the *SR* of a compound will be lower during colder deployments, because $K_{XAD/Gas}$ increases at lower temperatures. To fully explore this quantitatively would require additional calibrations of the XAD-PAS at temperatures that deviate substantially from those of the current study. Because of the wide seasonal temperature range in Toronto, the current calibration does however allow for some preliminary exploration of this issue, which will be described in a follow-up paper.

ASSOCIATED CONTENT

Supporting Information

The Supporting Information is available free of charge on the ACS Publications website at DOI: 10.1021/XXX. It contains additional tables, figures and text on the obtained data. The version of the PAS-SIM model used in this study is available in the supporting information.

AUTHOR INFORMATION

Corresponding Authors

*E-mail: faqiang.zhan@utoronto.ca, frank.wania@utoronto.ca, Telephone: +1-416-287-7225

ORCID:

Yuening Li: 0000-0001-7679-8440

Faqiang Zhan: 0000-0003-1065-2101

Chubashini Shunthirasingham: 0000-0003-0498-6519

Hayley Hung: 0000-0003-0719-8948

Frank Wania: 0000-0003-3836-0901

Notes

The authors declare no competing financial interest.

Acknowledgement

We are grateful to Rudy Boonstra for logistical help during field work. Financial support from a Grant and Contribution Agreement (GCXE20S008) with Environment and Climate Change Canada under the Whale Recovery Initiative and a Connaught scholarship to YL is gratefully acknowledged.

Literature Cited

(1) Bidleman, T. F. Atmospheric Processes. *Environ. Sci. Technol.* **1988**, *22*, 361–367.

(2) Lyche, J. L.; Rosseland, C.; Berge, G.; Polder, A. Human Health Risk Associated with Brominated Flame-Retardants (BFRs). *Environ. Int.* **2015**, *74*, 170–180.

(3) Androutsopoulos, V. P.; Hernandez, A. F.; Liesivuori, J.; Tsatsakis, A. M. A Mechanistic Overview of Health Associated Effects of Low Levels of Organochlorine and Organophosphorous Pesticides. *Toxicology* **2013**, *307*, 89–94.

(4) Letcher, R. J.; Bustnes, J. O.; Dietz, R.; Jenssen, B. M.; Jørgensen, E. H.; Sonne, C.; Verreault, J.; Vijayan, M. M.; Gabrielsen, G. W. Exposure and Effects Assessment of Persistent Organohalogen Contaminants in Arctic Wildlife and Fish. *Sci. Total Environ.* **2010**, *408*, 2995–3043.

(5) Oehme, M. Further Evidence for Long-Range Air Transport of Polychlorinated Aromates and Pesticides: North America and Eurasia to the Arctic. *Ambio* **1991**, *20*, 293–297.

(6) Patton, G. W.; Walla, M. D.; Bidleman, T. F.; Barrie, L. A. Polycyclic Aromatic and Organochlorine Compounds in the Atmosphere of Northern Ellesmere Island, Canada. *J. Geophys. Res. Atmos.* **1991**, *96* (D6), 10867–10877.

(7) Wania, F.; Shunthirasingham, C. Passive Air Sampling for Semi-Volatile Organic Chemicals. *Environ. Sci. Process. Impacts* **2020**, *22*, 1925–2002.

(8) Dobson, R.; Scheyer, A.; Rizet, A. L.; Mirabel, P.; Millet, M. Comparison of the Efficiencies of Different Types of Adsorbents at Trapping Currently Used Pesticides in the Gaseous Phase Using the Technique of High-Volume Sampling. *Anal. Bioanal. Chem.* **2006**, *386*, 1781–1789.

(9) Hayward, S. J.; Todd, G.; Wania, F. Comparison of Four Active and Passive Sampling Techniques for Pesticides in Air. *Environ. Sci. Technol.* **2010**, *44*, 3410–3416.

(10) Muir, D. C. G.; Segstro, M. D.; Welbourn, P. M.; Toom, D.; Eisenreich, S. J.; Macdonald, C. R.; Whelpdale, D. M. Patterns of Accumulation of Airborne Organochlorine

Contaminants in Lichens from the Upper Great Lakes Region of Ontario. *Environ. Sci. Technol.* **1993**, *27*, 1201–1210.

(11) Kylin, H.; Grimvall, E.; Oestman, C. Environmental Monitoring of Polychlorinated Biphenyls Using Pine Needles as Passive Samplers. *Environ. Sci. Technol.* **1994**, *28*, 1320–1324.

(12) Müller, J. F.; Hawker, D. W.; Connell, D. W.; Kömp, P.; McLachlan, M. S. Passive Sampling of Atmospheric SOCs Using Tristearin-Coated Fibreglass Sheets. *Atmos. Environ.* **2000**, *34*, 3525–3534.

(13) Wania, F.; Shen, L.; Lei, Y. D.; Teixeira, C.; Muir, D. C. G. Development and Calibration of a Resin-Based Passive Sampling System for Monitoring Persistent Organic Pollutants in the Atmosphere. *Environ. Sci. Technol.* **2003**, *37*, 1352–1359.

(14) Bidleman, T. F.; Olney, C. E. Chlorinated Hydrocarbons in the Sargasso Sea Atmosphere and Surface Water. *Science* **1974**, *183* (4124), 516–518.

(15) Bidleman, T. F.; Olney, C. E. High-Volume Collection of Atmospheric Polychlorinated Biphenyls. *Bull. Environ. Contam. Toxicol.* **1974**, *11*, 442–450.

(16) Bidleman, T. F.; Melymuk, L. Forty-Five Years of Foam: A Retrospective on Air Sampling with Polyurethane Foam. *Bull. Environ. Contam. Toxicol.* **2019**, *102*, 447–449.

(17) Zhao, D.; Little, J. C.; Cox, S. S. Characterizing Polyurethane Foam as a Sink for or Source of Volatile Organic Compounds in Indoor Air. *J. Environ. Eng.* **2004**, *130*, 983–989.

(18) Braun, T.; Navratil, J. D.; Farag, A. B. *Polyurethane Foam Sorbents in Separation Science*, 1st Editio.; CRC Press: Boca Raton, 1985.

(19) Kamprad, I.; Goss, K. U. Systematic Investigation of the Sorption Properties of Polyurethane Foams for Organic Vapors. *Anal. Chem.* **2007**, *79*, 4222–4227.

(20) Li, Y.; Wania, F. Partitioning between Polyurethane Foam and the Gas Phase: Data Compilation, Uncertainty Estimation and Implications for Air Sampling. *Environ. Sci. Process. Impacts* **2021**, *23*, 723–734.

(21) Li, Y.; Armitage, J. M.; Wania, F. Graphical Tools for the Planning and Interpretation of Polyurethane Foam Based Passive Air Sampling Campaigns. *Environ. Sci. Process. Impacts* **2022**, *24*, 414–425.

(22) Richard, J. J.; Fritz, J. S. Adsorption of Chlorinated Pesticides from River Water with XAD-2 Resin. *Talanta* **1974**, *21*, 91–93.

(23) Musty, P. R.; Nickless, G. Use of Amberlite XAD-4 for Extraction and Recovery of Chlorinated Insecticides and Polychlorinated Biphenyls from Water. *J. Chromatogr. A* **1974**, *89*, 185–190.

(24) Burnham, A. K.; Calder, G. V.; Fritz, J. S.; Junk, G. A.; Svec, H. J.; Willis, R. Identification and Estimation of Neutral Organic Contaminants in Potable Water. *Anal. Chem.* **1972**, *44*, 139–142.

(25) Bunn, W. W.; Deane, E. R.; Klein, D. W.; Kleopfer, R. D. Sampling and Characterization of Air for Organic Compounds. *Water. Air. Soil Pollut.* **1975**, *4*, 367–380.

(26) Chuang, J. C.; Wilson, N. K.; Hannan, S. W. Field Comparison of Polyurethane Foam

and XAD-2 Resin for Air Sampling for Polynuclear Aromatic Hydrocarbons. *Environ. Sci. Technol.* **1987**, *21*, 798–804.

(27) Gong, P.; Wang, X.; Liu, X.; Wania, F. Field Calibration of XAD-Based Passive Air Sampler on the Tibetan Plateau: Wind Influence and Configuration Improvement. *Environ. Sci. Technol.* **2017**, *51*, 5642–5649.

(28) Okeme, J. O.; Yang, C.; Abdollahi, A.; Dhal, S.; Harris, S. A.; Jantunen, L. M.; Tsirlin, D.; Diamond, M. L. Passive Air Sampling of Flame Retardants and Plasticizers in Canadian Homes Using PDMS, XAD-Coated PDMS and PUF Samplers. *Environ. Pollut.* **2018**, *239*, 109–117.

(29) Okeme, J. O.; Saini, A.; Yang, C.; Zhu, J.; Smedes, F.; Klánová, J.; Diamond, M. L. Calibration of Polydimethylsiloxane and XAD-Pocket Passive Air Samplers (PAS) for Measuring Gas- and Particle-Phase SVOCs. *Atmos. Environ.* **2016**, *143*, 202–208.

(30) Shoeib, M.; Harner, T.; Sum, C. L.; Lane, D.; Zhu, J. Sorbent-Impregnated Polyurethane Foam Disk for Passive Air Sampling of Volatile Fluorinated Chemicals. *Anal. Chem.* **2008**, *80*, 675–682.

(31) Ramírez-Restrepo, A.; Hayward, S. J.; Armitage, J. M.; Wania, F. Evaluating the PAS-SIM Model Using a Passive Air Sampler Calibration Study for Pesticides. *Environ. Sci. Process. Impacts* **2015**, *17*, 1228–1237.

(32) Gouin, T.; Wania, F.; Ruepert, C.; Castillo, L. E. Field Testing Passive Air Samplers for Current Use Pesticides in a Tropical Environment. *Environ. Sci. Technol.* **2008**, *42*, 6625–6630.

(33) Shunthirasingham, C.; Mmereki, B. T.; Masamba, W.; Oyiliagu, C. E.; Lei, Y. D.; Wania, F. Fate of Pesticides in the Arid Subtropics, Botswana, Southern Africa. *Environ. Sci. Technol.* **2010**, *44*, 8082–8088.

(34) Armitage, J. M.; Hayward, S. J.; Wania, F. Modeling the Uptake of Neutral Organic Chemicals on XAD Passive Air Samplers under Variable Temperatures, External Wind Speeds and Ambient Air Concentrations (PAS-SIM). *Environ. Sci. Technol.* **2013**, *47*, 13546–13554.

(35) Ellickson, K. M.; McMahon, C. M.; Herbrandson, C.; Krause, M. J.; Schmitt, C. M.; Lippert, C. J.; Pratt, G. C. Analysis of Polycyclic Aromatic Hydrocarbons (PAHs) in Air Using Passive Sampling Calibrated with Active Measurements. *Environ. Pollut.* **2017**, *231*, 487–496.

(36) Gawor, A.; Shunthirasingham, C.; Hayward, S. J.; Lei, Y. D.; Gouin, T.; Mmereki, B. T.; Masamba, W.; Ruepert, C.; Castillo, L. E.; Shoeib, M.; et al. Neutral Polyfluoroalkyl Substances in the Global Atmosphere. *Environ. Sci. Process. Impacts* **2014**, *16*, 404–413.

(37) Krogseth, I. S.; Zhang, X.; Lei, Y. D.; Wania, F.; Breivik, K. Calibration and Application of a Passive Air Sampler (XAD-PAS) for Volatile Methyl Siloxanes. *Environ. Sci. Technol.* **2013**, *47*, 4463–4470.

(38) Melymuk, L.; Bohlin, P.; Sáňka, O.; Pozo, K.; Klánova, J.; Sáňka, O.; Pozo, K.; Klánová, J. Current Challenges in Air Sampling of Semivolatile Organic Contaminants: Sampling Artifacts and Their Influence on Data Comparability. *Environ. Sci. Technol.* **2014**, *48*, 14077–14091.

(39) Wania, F.; Warner, N. A.; McLachlan, M. S.; Durham, J.; Miøen, M.; Lei, Y. D.; Xu, S.

Seasonal and Latitudinal Variability in the Atmospheric Concentrations of Cyclic Volatile Methyl Siloxanes in the Northern Hemisphere. *Environ. Sci. Process. Impacts* **2023**, *25*, 496–506.

(40) Hayward, S. J.; Lei, Y. D.; Wania, F. Sorption of a Diverse Set of Organic Chemical Vapors onto XAD-2 Resin: Measurement, Prediction and Implications for Air Sampling. *Atmos. Environ.* **2011**, *45*, 296–302.

(41) Ulrich, N., Endo, S., Brown, T.N., Watanabe, N., Bronner, G., Abraham, M.H., Goss, K.-U. UFZ-LSER database v 3.2.1 [Internet] http://www.ufz.de/lserd (accessed Jul 13, 2022).

(42) Bohlin, P.; Audy, O.; Škrdlíková, L.; Kukučka, P.; Přibylová, P.; Prokeš, R.; Vojta, Š.; Klánová, J. Outdoor Passive Air Monitoring of Semi Volatile Organic Compounds (SVOCs): A Critical Evaluation of Performance and Limitations of Polyurethane Foam (PUF) Disks. *Environ. Sci. Process. Impacts* **2014**, *16*, 433–444.

(43) Khairy, M. A.; Lohmann, R. Field Calibration of Low Density Polyethylene Passive Samplers for Gaseous POPs. *Environ. Sci. Process. Impacts* **2014**, *16*, 414–421.

(44) Ockenden, W. A.; Corrigan, B. P.; Howsam, M.; Jones, K. C. Further Developments in the Use of Semipermeable Membrane Devices as Passive Air Samplers: Application to PCBs. *Environ. Sci. Technol.* **2001**, *35*, 4536–4543.

(45) Bartkow, M. E.; Hawker, D. W.; Kennedy, K. E.; Müller, J. F. Characterizing Uptake Kinetics of PAHs from the Air Using Polyethylene-Based Passive Air Samplers of Multiple Surface Area-to-Volume Ratios. *Environ. Sci. Technol.* **2004**, *38*, 2701–2706.

(46) Moeckel, C.; Harner, T.; Nizzetto, L.; Strandberg, B.; Lindroth, A.; Jones, K. C. Use of Depuration Compounds in Passive Air Samplers: Results from Active Sampling-Supported Field Deployment, Potential Uses, and Recommendations. *Environ. Sci. Technol.* **2009**, *43*, 3227–3232.

(47) Zhang, X.; Wong, C.; Lei, Y. D.; Wania, F. Influence of Sampler Configuration on the Uptake Kinetics of a Passive Air Sampler. *Environ. Sci. Technol.* **2012**, *45*, 397–403.

(48) Zhang, X.; Brown, T. N.; Ansari, A.; Yeun, B.; Kitaoka, K.; Kondo, A.; Lei, Y. D.; Wania, F. Effect of Wind on the Chemical Uptake Kinetics of a Passive Air Sampler. *Environ. Sci. Technol.* **2013**, *47*, 7868–7875.

(49) Schwarzenbach, R. P.; Gschwend, P. M.; Imboden, D. M. *Environmental Organic Chemistry*, 2nd ed.; John Wiley & Sons, Inc.: Hoboken, NJ, USA, 2002.

(50) Melymuk, L.; Bohlin-Nizzetto, P.; Prokeš, R.; Kukučka, P.; Klánová, J. Sampling Artifacts in Active Air Sampling of Semivolatile Organic Contaminants: Comparing Theoretical and Measured Artifacts and Evaluating Implications for Monitoring Networks. *Environ. Pollut.* **2016**, *217*, 97–106.

(51) Wu, R.; Backus, S.; Basu, I.; Blanchard, P.; Brice, K.; Dryfhout-Clark, H.; Fowlie, P.; Hulting, M.; Hites, R. Findings from Quality Assurance Activities in the Integrated Atmospheric Deposition Network. *J. Environ. Monit.* **2009**, *11*, 277–296.

(52) Zhang, X.; Wania, F. Modeling the Uptake of Semivolatile Organic Compounds by Passive Air Samplers: Importance of Mass Transfer Processes within the Porous Sampling Media. *Environ. Sci. Technol.* **2012**, *46*, 9563–9570.

(53) Daly, G. L., Y. D. Lei, D. C. G. Muir, L. E. Castillo, F. Wania. Polycyclic Aromatic Hydrocarbons in Costa Rican Air and Soil: A Tropical/Temperate Comparison.

Atmos. Environ. **2007**, *41*, 7339–7350.

(54 Westgate, J. N., C. Shunthirasingham, C. E. Oyiliagu, H. von Waldow, F. Wania. Three Methods for Quantifying Proximity of Air Sampling Sites to Spatially Resolved Emissions of Semivolatile Organic Contaminants. *Atmos. Environ.* **2010**, *44*, 4380–4387.

(55) Holt, E.; Bohlin-Nizzetto, P.; Borůvková, J.; Harner, T.; Kalina, J.; Melymuk, L.; Klánová, J. Using Long-Term Air Monitoring of Semi-Volatile Organic Compounds to Evaluate the Uncertainty in Polyurethane-Disk Passive Sampler-Derived Air Concentrations. *Environ. Pollut.* **2017**, *220*, 1100–1111.

(56) Zhang, X.; Hoang, M.; Lei, Y. D.; Wania, F. Exploring the Role of the Sampler Housing in Limiting Uptake of Semivolatile Organic Compounds in Passive Air Samplers. *Environ. Sci. Process. Impacts* **2015**, *17*, 2006–2012.

(57) Zhang, X.; Tsurukawa, M.; Nakano, T.; Lei, Y. D.; Wania, F. Sampling Medium Side Resistance to Uptake of Semivolatile Organic Compounds in Passive Air Samplers. *Environ. Sci. Technol.* **2011**, *45*, 10509–10515.

(58) Li, Y.; Xiong, S.; Hao, Y.; Yang, R.; Zhang, Q.; Wania, F.; Jiang, G. Organophosphate Esters in Arctic Air from 2011 to 2019: Concentrations, Temporal Trends, and Potential Sources. *J. Hazard. Mater.* **2022**, *434*, 128872.

Supporting information for

Field Calibration and PAS-SIM Model Evaluation of the XAD-based Passive Air Sampler for Semi-volatile Organic Compounds

Yuening Li,[1] Faqiang Zhan,[1*] Ying Duan Lei,[1] Chubashini Shunthirasingham,[2] Hayley Hung,[2] Frank Wania[1*]

1. *Department of Physical and Environmental Sciences, University of Toronto Scarborough, 1265 Military Trail, Toronto, Ontario, Canada M1C 1A4*

2. *Air Quality Processes Research Section, Environment and Climate Change Canada, 4905 Dufferin Street, Toronto, Ontario, Canada M3H 5T4*

[*]Corresponding authors: faqiang.zhan@utoronto.ca, frank.wania@utoronto.ca, +1-416-287-7225

Summary: 21 pages, 1 page of text, 6 figures, 7 tables

Content

Text S1 Sample Treatment and Analysis

Accelerated Solvent Extraction (ASE). Detailed information on the ASE extraction is as follows: temperature, 75 °C; purge time, 240 seconds; 3 static cycles; static time, 6 minutes; rinse volume, 100% cell volume.

Halogenated methoxybenzene, industrial organochlorines, metabolic by-products of pesticides and organochlorine Pesticides (OCPs) analysis. These chemicals in the sample extracts were analyzed using an Agilent 7000A triple quadrupole mass spectrometer (MS/MS) connected to an Agilent 7890A gas chromatograph (GC) using electron ionization (EI) mode. 2 μL of each extract were injected into a capillary DB-5 column (Agilent J&W Scientific, 30 m length, 0.25 mm inside diameter, and 0.25 μm film thickness) using pulsed splitless mode at 250 ℃. Helium was used as a carrier gas at a flow rate of 1 mL min^{-1}. The GC oven temperature program was as follows: oven temperature was initially set as 80 ℃, 20 ℃ min^{-1} to 160 ℃, then raised to 230 ℃ at 3 ℃ min^{-1}, finally reached 300 ℃ at 20 ℃ min^{-1} and held for 10 minutes. The ion source and interface temperatures were set as 250 ℃ and 280 ℃, respectively.

Organophosphate Esters (OPEs) analysis. OPEs were analyzed using the same instrument, column, and helium carrier gas setting as those for OCPs analysis. 2 μL of each extract were injected into the GC column using pulsed splitless mode at 200 ℃. The GC oven temperature program was as follows: the oven temperature was initially held at 90 ℃ for 1 minute, then raised to 200 ℃ at 15 ℃ min^{-1}, held for 3 minutes, and then raised to 250 ℃ at 5 ℃ min^{-1}, finally raised to 300 ℃ at 15 ℃ min^{-1} and held for 3 minutes. The ion source and interface temperatures were identical to those for OCP analysis.

Halogenated flame retardants (HFRs) analysis. Quantification of HFRs was completed using GC-MS/MS (Thermo Scientific Trace 1310 GC coupled to a TSQ 8000 Evo Triple Quadrupole MS/MS) in EI mode. 2 μL of each extract were injected using a TriPlus RSH autosampler in PTV splitless mode (80 ℃ for 0.05 minutes then heading up to 280 ℃ at 14.5 ℃ $second^{-1}$). A Rxi-5Sil MS column (Restek: 15 m length, 0.25 mm inside diameter, and 0.1 μm film thickness) was used for the separation, with helium as the carrier gas at a flow rate of 1.5 mL min-^{1}. The temperatures of the inlet and interface were set at 280 ℃ and 290 ℃, respectively. The GC oven temperature program was set to start at 90 ℃, hold for 1 minute, ramp to 250 ℃ at 18 ℃ min^{-1}, then further ramp to 280 at 10 ℃ min^{-1}, and finally, ramp to 310 ℃ at 30 ℃ min^{-1} and held for 6 minutes.

Neutral per- and polyfluoroalkyl compounds (nPFAS) analysis. The nPFASs were analyzed using an Agilent 5977A MS connected to a 7890B GC. The GC-MS was operated in selected ion monitoring mode under positive chemical ionization. Details on the operation parameters of the instrumental analysis and the monitoring ions for each nPFASs have been reported in the paper by Gawor et al.[1]

Table S1. List of spike, injection, and native standards, their abbreviations, and suppliers

Chemicals	Abbreviation	Supplier
Spike Standards		
Labeled Organophosphate Esters (OPEs)		
Triethyl Phosphate-d_{15}	d_{15}-TEP	Wellington Lab (Canada)
Tri-n-propyl Phosphate-d_{21}	d_{21}-TPrP	Wellington Lab (Canada)
Triphenyl Phosphate-d_{15}	d_{15}-TPhP	Wellington Lab (Canada)
Tris(2-chloroethyl) phosphate-d_{12}	d_{12}-TCEP	Wellington Lab (Canada)
Tris(2-butoxy-[$^{13}C_2$]-ethyl) phosphate	$^{13}C_2$-TBEP	Wellington Lab (Canada)
Tris(1,3-dichloro-2-propyl) phosphate-d_{15}	d_{15}-TDCPP	Wellington Lab (Canada)
Tributyl Phosphate-d_{27}	d_{27}-TBP	Cambridge Iso. Lab. (U.S.)
Labeled Organochlorine Pesticides (OCPs)		
$^{13}C_6$-Pentachloroanisole	$^{13}C_6$-PCA	Cambridge Iso. Lab. (U.S.)
$^{13}C_6$-Pentachlorobenzene	$^{13}C_6$-PeCB	Cambridge Iso. Lab. (U.S.)
$^{13}C_6$-alpha-Hexachlorocyclohexane	$^{13}C_6$-α-HCH	Cambridge Iso. Lab. (U.S.)
$^{13}C_6$-Hexachlorobenzene	$^{13}C_6$-HCB	Cambridge Iso. Lab. (U.S.)
$^{13}C_{10}$-Heptachlor	$^{13}C_{10}$-HEP	Cambridge Iso. Lab. (U.S.)
$^{13}C_{10}$-Trans-chlordane	$^{13}C_{10}$-TC	Cambridge Iso. Lab. (U.S.)
$^{13}C_{12}$-Dichlorodiphenyldichloroethylene	$^{13}C_{12}$-PPDDE	Cambridge Iso. Lab. (U.S.)
$^{13}C_9$-Endosulfan II	$^{13}C_9$-Endo II	Cambridge Iso. Lab. (U.S.)
$^{13}C_{12}$-Clofenotane	$^{13}C_{12}$-p,p-DDT	Cambridge Iso. Lab. (U.S.)
Labeled Halogenated Flame Retardants (HFRs)		
$^{13}C_{12}$-2,4,4'-Tribrominated diphenyl ether (BDE)	$^{13}C_{12}$-BDE 28	Cambridge Iso. Lab. (U.S.)
$^{13}C_{12}$-2,2',4,4'-TetraBDE	$^{13}C_{12}$-BDE 47	Cambridge Iso. Lab. (U.S.)
$^{13}C_{12}$-2,2',4,4',5-PentaBDE	$^{13}C_{12}$-BDE-99	Cambridge Iso. Lab. (U.S.)
$^{13}C_{12}$-2,2',3,4,4',6-HexaBDE	$^{13}C_{12}$-BDE 139	Cambridge Iso. Lab. (U.S.)
$^{13}C_{12}$-2,2',3,4,4',5,5'-HeptaBDE	$^{13}C_{12}$-BDE180	Wellington Lab (Canada)
2,3,3',4,4',5,5',6-OctaBDE	BDE205	Cambridge Iso. Lab. (U.S.)
$^{13}C_{12}$-DecaBDE	$^{13}C_{12}$-BDE209	Cambridge Iso. Lab. (U.S.)
$^{13}C_6$-Pentabromobenzene	$^{13}C_6$-PBBz	Wellington Lab (Canada)
$^{13}C_6$-Hexabromobenzene	$^{13}C_6$-HBBz	Wellington Lab (Canada)
2-Ethylhexyl-d_{17}-2,3,4,5-tetrabromo[$^{13}C_6$]benzoate	$^{13}C_6$-EHTBB	Wellington Lab (Canada)
Bis(2-ethylhexyl-d_{17})tetrabromo[$^{13}C_6$]phthalate	$^{13}C_6$-BEHTBP	Wellington Lab (Canada)
$^{13}C_6$-1,2-Bis(2,4,6-tribromophenoxy)ethane	$^{13}C_6$-BTBPE	Wellington Lab (Canada)
$^{13}C_{10}$-Dechlorane Plus Anti	$^{13}C_{10}$-anti-DP	Cambridge Iso. Lab. (U.S.)
$^{13}C_{14}$-1,2-Bis(pentabromophenyl)ethane	$^{13}C_{14}$-DBDPE	Wellington Lab (Canada)
$^{13}C_{10}$-Dechlorane 602	$^{13}C_{10}$-Dec-602	Cambridge Iso. Lab. (U.S.)
Labeled neutral per- and polyfluoroalkyl compounds		
2-Perfluorohexyl (1,1-2 H2 ,1,2-$^{13}C_2$)ethanol	$^{13}C_2$-6:2 FTOH	Wellington Lab (Canada)
2-Perfluorooctyl (1,1-2 H2 ,1,2-$^{13}C_2$)ethanol	$^{13}C_2$-8:2 FTOH	Wellington Lab (Canada)
2-Perfluorodecyl (1,1-2 H2 ,1,2-$^{13}C_2$)ethanol	$^{13}C_2$-10:2 FTOH	Wellington Lab (Canada)
Perfluoro-1-[$^{13}C_8$]octanesulfonamide	$^{13}C_8$-FOSA-I	Wellington Lab (Canada)
2-(N-methyl-d_3-perfluoro-1-octanesulfonamido)ethan-d_4-ol	d_7-N-MeFOSE-M	Wellington Lab (Canada)
2-(N-ethyl-d_5-perfluoro-1-octanesulfonamido)ethan- d_4-ol	d_9-N-EtFOSE-M	Wellington Lab (Canada)
N-ethyl-d_5-perfluoro-1-octanesulfonamide	d_5-N-EtFOSA-M	Wellington Lab (Canada)
N-methyl-d_3-perfluoro-1-octanesulfonamide	d_3-N-MeFOSA-M	Wellington Lab (Canada)

Injection Standards		
Triamyl Phosphate	TAP	TCI America (U.S.)
$^{13}C_{12}$-2,3,3',4,4'-Pentacb	$^{13}C_{12}$-PCB105	Cambridge Iso. Lab. (U.S.)
$^{13}C_{12}$-2,2',3,4,4',5,5'-Heptacb	$^{13}C_{12}$-PCB180	Cambridge Iso. Lab. (U.S.)
$^{13}C_{8}$-Mirex	N/A	Cambridge Iso. Lab. (U.S.)
N,N-dimethylperfluoro-1-octanesulfonamide	NNMe2FOSA	Wellington Lab (Canada)
Native Standards		
Halogenated methoxybenzene		
2, 4-dibromoanisole	DBA	Cambridge Iso. Lab. (U.S.)
2,4,6-Tribromoanisole	TBA	Cambridge Iso. Lab. (U.S.)
Pentachloroanisole	PCA	AccuStandard (U.S.)
Tetrachloroveratrole	TeCV	AccuStandard (U.S.)
1,4-Dimethoxytetrachlorobenzene	DAME	BOC Sciences (U.S.)
Industrial organochlorines		
Hexachlorobutadiene	HCBD	AccuStandard (U.S.)
Hexachlorocyclopentadiene	HCCPD	AccuStandard (U.S.)
Pentachloronitrobenzene	PCNB	Cambridge Iso. Lab. (U.S.)
Pentachlorobenzene	PeCB	Cambridge Iso. Lab. (U.S.)
Hexachlorobenzene	HCB	Cambridge Iso. Lab. (U.S.)
Tetrachloronitrobenzene	TCNB	AccuStandard (U.S.)
Metabolic by-products of pesticides		
Pentachloroaniline	PCAN	AccuStandard (U.S.)
Pentachlorothioanisole	PCTA	AccuStandard (U.S.)
Oxychordane	Oxchlord	Cambridge Iso. Lab. (U.S.)
Organochlorine Pesticides (OCPs)		
Alpha-hexachlorocyclohexane	α-HCH	AccuStandard (U.S.)
Beta-hexachlorocyclohexane	β-HCH	AccuStandard (U.S.)
Gamma-hexachlorocyclohexane	γ-HCH	AccuStandard (U.S.)
Delta-hexachlorocyclohexane	δ-HCH	Cambridge Iso. Lab. (U.S.)
Dichlorodiphenyldichloroethylene	pp'-DDE	AccuStandard (U.S.)
Ethyl 2,4-Dioxo-4-(2-Pyridinyl)Butanoate	op'-DDD	Cambridge Iso. Lab. (U.S.)
2,2-(2-Chlorophenyl-4'-Chlorophenyl)-1,1-Dichloroethene	o,p-DDE	Cambridge Iso. Lab. (U.S.)
1,1-dichloro-2,2 bis(p-chlorophenyl) ethane	pp'-DDD	AccuStandard (U.S.)
1,1,1-trichloro-2-(o-chlorophenyl)-2-(p-chlorophenyl) ethane	op'-DDT	AccuStandard (U.S.)
1,1,1-trichloro-2,2-bis(p-chlorophenyl ethane	pp'-DDT	AccuStandard (U.S.)
Aldrin	N/A	AccuStandard (U.S.)
Cis-chlordane	CC	AccuStandard (U.S.)
Dieldrin	N/A	AccuStandard (U.S.)
Endosulfan I (alpha)	α-Endo	AccuStandard (U.S.)
Endosulfan II (beta)	β-Endo	AccuStandard (U.S.)
Endosulfan Sulfate	Endo S	AccuStandard (U.S.)
Endrin	N/A	AccuStandard (U.S.)
Heptachlor	HEPT	Cambridge Iso. Lab. (U.S.)
Heptachlor exo-epoxide	Hepx	AccuStandard (U.S.)
1-methoxy-4-[2,2,2-trichloro-1-(4-Methoxyphenyl)ethyl]benzene	Methoxychlor	AccuStandard (U.S.)
Mirex	N/A	AccuStandard (U.S.)
Photomirex	N/A	AccuStandard (U.S.)

Trans-chlordane	TC	AccuStandard (U.S.)
Trans-nonachlor	TN	AccuStandard (U.S.)
OPEs		
Tri-ethyl phosphate	TEP	Wellington Lab (Canada)
Tri-propyl phosphate	TPrP	Wellington Lab (Canada)
Tri-n-butyl phosphate	TBP	Wellington Lab (Canada)
Tris(2-chloroethyl) phosphate	TCEP	Wellington Lab (Canada)
Tris(1-chloro-2-propyl) phosphate	TCPP	Wellington Lab (Canada)
Tris(1,3-dichloro-2-propyl) phosphate	TDCPP	Wellington Lab (Canada)
Tris (phenyl)phosphate	TPhP	Wellington Lab (Canada)
Tris (2-butoxyethyl) phosphate	TBEP	Wellington Lab (Canada)
2-ethylhexyl-diphenyl phosphate	EHDPP	Wellington Lab (Canada)
Tris (2-ethylhexyl) phosphate	TEHP	Wellington Lab (Canada)
Tri-o-tolyl phosphate	ToTP	Wellington Lab (Canada)
Tri-m-tolyl phosphate	TmTP	Wellington Lab (Canada)
Tri-p-tolyl phosphate	TpTP	Wellington Lab (Canada)
Tris(2-isopropylphenyl) phosphate	T2IPP	Wellington Lab (Canada)
Tris(3,5-dimethylphenyl) phosphate	T35DMPP	Wellington Lab (Canada)
Tris(2,3-dibromopropyl) phosphate	TDBPP	Wellington Lab (Canada)
HFRs		
Allyl-2,4,6-tribromophenyl ether	ATE	Wellington Lab (Canada)
Alpha-1,2-Dibromo-4-(1,2-dibromoethyl)cyclohexane	α-TBECH	Wellington Lab (Canada)
Beta-1,2-Dibromo-4-(1,2-dibromoethyl)cyclohexane	β-TBECH	Wellington Lab (Canada)
2-bromoallyl-2,4,6-tribromophenyl ether	BATE	Wellington Lab (Canada)
Pentabromobenzene	PBBz	Wellington Lab (Canada)
Pentabromotoluene	PBT	Wellington Lab (Canada)
Pentabromoethylbenzene	PBEB	Wellington Lab (Canada)
Dibromopropyl-2,4,6-tribromophenyl ether	DPTE	Wellington Lab (Canada)
Hexabromobenzene	HBB	Wellington Lab (Canada)
Dechlorane 602	Dec-602	Wellington Lab (Canada)
2-ethylhexyl-2,3,4,5-tetrabromobenzoate	EHTBB	Wellington Lab (Canada)
Dechlorane 604	DEC604	Wellington Lab (Canada)
Bis(2-ethylhexyl)-3,4,5,6-tetrabromo-phthalate	BEHTBP	Wellington Lab (Canada)
Syn-dechlorane plus	S-DP	Wellington Lab (Canada)
Anti-dechlorane plus	a-DP	Wellington Lab (Canada)
Decabromodiphenyl ethane	DBDPE	Wellington Lab (Canada)
1,2-Bis(2,4,6-tribromophenoxy) ethane	BTBPE	Wellington Lab (Canada)
2,2',4- Tribrominated diphenyl ether (BDE)	BDE 17	Wellington Lab (Canada)
2,4,4'-TriBDE	BDE 28	Wellington Lab (Canada)
2,2',4,4'-TetraBDE	BDE 47	Wellington Lab (Canada)
2,2',4,5'-TetraBDE	BDE 49	Wellington Lab (Canada)
2,3',4,4'-TetraBDE	BDE 66	Wellington Lab (Canada)
2,3',4',6-TetraBDE	BDE 71	Wellington Lab (Canada)
2,2',3,4,4'-PentaBDE	BDE 85	Wellington Lab (Canada)
2,2',4,4',5-PentaBDE	BDE 99	Wellington Lab (Canada)
2,2',4,4',6-PentaBDE	BDE 100	Wellington Lab (Canada)
2,2',3,4,4',5'-HexaBDE	BDE 138	Wellington Lab (Canada)
2,2',4,4',5,5'-HexaBDE	BDE 153	Wellington Lab (Canada)

2,2',4,4',5,6'-HexaBDE	BDE 154	Wellington Lab (Canada)
2,2',3,4,4',5',6-HeptaBDE	BDE 183	Wellington Lab (Canada)
2,3,3',4,4',5,6-HeptaBDE	BDE 190	Wellington Lab (Canada)
DecaBDE	BDE 209	Wellington Lab (Canada)
Neutral per- and polyfluoroalkyl compounds		
2-(perfluorohexyl)ethyl methacrylate	6:2 FTA	Cambridge Iso. Lab. (U.S.)
Perfluoro hexyl- ethanol	6:2 FTOH	Cambridge Iso. Lab. (U.S.)
2-(perfluorooctyl)ethyl acrylate	8:2 FTA	Cambridge Iso. Lab. (U.S.)
Perfluoro octyl- ethanol	8:2 FTOH	Cambridge Iso. Lab. (U.S.)
2-(perfluorodecyl)ethyl acrylate	10:2 FTA	Cambridge Iso. Lab. (U.S.)
Perfluoro decyl- ethanol	10:2 FTOH	Cambridge Iso. Lab. (U.S.)
N ethyl perfluoro- 1-octane sulfonamide	EtFOSA	Cambridge Iso. Lab. (U.S.)
N-Methylperfluoro-1-butanesulfonamide	MeFBSA	Wellington Lab (Canada)
N-methylperfluoro-1-octansulfonamide	MeFOSA	Cambridge Iso. Lab. (U.S.)
N-Methylperfluorooctanesulfonamidoethanol	MeFOSE	Cambridge Iso. Lab. (U.S.)
N-Ethylperfluorooctanesulfonamidoethanol	EtFOSE	Cambridge Iso. Lab. (U.S.)
Perfluorooctanesulfonamide	FOSA	Cambridge Iso. Lab. (U.S.)
Perfluorohexanesulfonamide	FHxSA	Cambridge Iso. Lab. (U.S.)
Perfluorobutanesulfonamide	FBSA	Cambridge Iso. Lab. (U.S.)

Table S2. Recoveries of spiking standards used for the quantification of native chemicals

	Recovery Rates (%)	
	Passive air sample (PAS)	**Active air sample (AAS)**
Labeled OPEs		
d_{15}-TEP	42.2 ± 18.7	23.3 ± 20.8
d_{21}-TPrP	82.3 ± 38.9	143.8 ± 14.5
d_{15}-TPhP	160.5 ± 23.3	162.6 ± 41.4
d_{12}-TCEP	76.4 ± 12.5	111.6 ± 29.5
$^{13}C_2$-TBEP	39.8 ± 17.1	255.3 ± 41.9
d_{15}-TDCPP	197.1 ± 26.7	147.7 ± 26.1
d_{27}-TBP	84.9 ± 16.4	167.0 ± 18.4
Labeled OCPs		
$^{13}C_6$-PCA	80.4 ± 6.8	84.3 ± 12.6
$^{13}C_6$-PeCBz	62.1 ± 6.7	76.9 ± 16.8
$^{13}C_6$-α-HCH	75.7 ± 6.3	105.2 ± 7.6
$^{13}C_6$-HCB	71.7 ± 5.9	85.3 ± 17.8
$^{13}C_{10}$-Heptachlor	87.9 ± 7.2	225.4 ± 27.0
$^{13}C_{10}$-TC	98.2 ± 9.9	104.6 ± 12.7
$^{13}C_{12}$-PPDDE	117.9 ± 20.7	125.1 ± 26.6
$^{13}C_9$-Endo II	90.2 ± 5.4	110.0 ± 12.7
$^{13}C_{12}$-p,p-DDT	175.3 ± 16.7	66.4 ± 28.9
Labeled HFRs		
$^{13}C_{12}$-BDE 28	102.2 ± 10.9	120.4 ± 12.4
$^{13}C_{12}$-BDE 47	103.6 ± 9.8	109.7 ± 12.0
$^{13}C_{12}$-BDE-99	113.6 ± 16.5	112.2 ± 11.5
$^{13}C_6$-PBBz	96.7 ± 15.9	112.2 ± 11.4
Labeled nPFASs		
d-N-MeFOSA-M	77.1 ± 25.8	60.9 ± 12.0

Table S3. The list of reliably detected target chemicals, their properties, and method detection limits (MDLs) for passive air samples (PASs) and active air samples (AASs)

Chemicals	Abbreviation	$\Delta U_{XAD/air}$ (kJ/mol) [1]	MW (g/mol)	MV (cm^3)[2]	Diffusivity (m^2/h)	MDL for PAS (ng/sample)	MDL for AAS (pg/m^3)
Hexachlorobutadiene	HCBD	-35	260.8	149	0.023	0.41	1.07
Pentachlorobenzene	PeCB	-38	250.3	149	0.023	0.07	0.27
2,4,6-Tribromoanisole	TBA	-37	344.8	153	0.022	0.12	0.62
α -hexachlorocyclohexane	α-HCH	-39	290.8	183	0.021	0.01	0.06
Tetrachloroveratrole	TeCV	-39	275.9	185	0.021	0.02	0.19
Hexachlorobenzene	HCB	-38	284.8	161	0.022	0.06	0.45
1,2,4,5-tetrachloro-3,6-Dimethoxybenzene	DAME	-40	275.9	185	0.021	0.04	0.72
Pentachloroanisole	PCA	-39	280.4	173	0.021	0.05	0.44
γ-hexachlorocyclohexane	γ-HCH	-39	290.8	183	0.021	0.01	0.27
δ-hexachlorocyclohexane	δ-HCH	-39	290.8	183	0.021	0.01	0.02
Heptachlor	Heptachlor	-42	373.3	208	0.019	0.02	0.10
Trans-chlordane	TC	-40	409.8	226	0.019	0.09	0.78
Cis-chlordane	CC	-41	409.8	226	0.019	0.02	0.24
Trans-nonachlor	TN	-40	444.2	238	0.018	0.01	0.09
Dieldrin	Dieldrin	-43	380.9	206	0.019	0.03	0.04
Dichlorodiphenyldichloroethylene	pp'-DDE	-44	318.0	227	0.019	0.11	0.03
Tripropyl phosphate	TPrP	-40	224.2	220	0.019	0.08	0.44
Tributyl phosphate	TBP	-43	266.3	270	0.017	0.18	0.10
Tris(2‑chloroethyl) phosphate	TCEP	-41	285.5	205	0.020	0.62	5.41
Tris(1-chloro-2-propyl) phosphate	TCPP	-40	224.2	220	0.019	0.11	0.87
Tris (phenyl)phosphate	TPhP	-47	326.3	258	0.018	0.29	0.94
Tris (2-ethylhexyl) phosphate	TEHP	-54	434.6	469	0.013	0.10	0.91
α-1,2-dibromo-4-(1,2-dibromoethyl)cyclohexane	α-TBECH	-40	427.8	197	0.020	0.02	0.04
β-1,2-dibromo-4-(1,2-dibromoethyl)cyclohexane	β-TBECH	-40	427.8	197	0.020	0.02	0.04
2,2',4,4'-tetrabromodiphenyl ether	BDE-47	-44	485.8	225	0.018	0.02	0.05
2-(perfluorodecyl)ethanol	10:2 FTOH	-48	564.1	339	0.015	0.40	0.74

[1] The internal energies of phase transfer between XAD and air were calculated based on poly parameter free energy relationships (ppLFERs) in the UFZ-LSER

[2] The molecular volumes were obtained from CompTox Chemicals Dashboard of United States Environmental Protection Agency.

Table S4. The effective sampling volumes of 26 chemicals during the one-year deployment period

	Effective sampling volumes of XAD-based passive air samplers during the sampling periods (m^3)											
	28 days	56 days	84 days	112 days	140 days	168 days	196 days	224 days	252 days	280 days	308 days	336 days
HCBD	9.1	14.4	19.6	38.6	57.7	77.4	102.7	112.2	117.1	143.3	187.8	172.6
PeCB	8.0	16.1	23.0	38.2	51.1	68.6	89.0	83.1	90.9	114.1	153.4	160.9
TBA	8.0	14.9	23.3	35.3	51.3	62.0	87.0	80.2	86.1	111.6	149.7	160.2
α-HCH	11.9	22.0	33.3	46.2	53.7	68.6	92.7	86.6	94.1	116.8	157.7	161.5
TeCV	7.2	12.2	19.8	32.3	33.3	41.2	46.2	55.3	65.5	70.2	93.6	107.0
HCB	8.0	14.4	22.6	39.6	46.7	56.9	79.8	78.8	87.0	105.7	141.9	159.5
DAME	8.9	15.6	22.5	37.7	43.7	53.0	66.1	62.7	69.3	82.8	109.0	126.9
PCA	8.2	17.9	22.3	39.6	46.2	56.3	70.8	69.0	74.6	99.9	128.5	136.7
γ-HCH	6.9	13.7	19.5	41.1	56.2	67.2	91.3	70.7	92.3	86.9	117.5	124.1
δ-HCH	9.0	9.6	20.7	35.4	50.3	53.8	75.1	72.5	125.8	(222.3)	(267.3)	(187.7)
Heptachlor	10.7	16.1	20.7	47.1	45.8	83.7	87.1	98.1	75.5	97.2	99.1	105.3
TC	N.D.	30.4	20.6	49.8	88.8	70.4	88.5	73.5	76.5	104.3	120.4	127.0
CC	7.6	22.1	24.7	44.3	58.7	76.9	79.7	79.8	116.6	150.7	163.2	174.4
TN	20.2	18.6	29.2	51.9	61.4	85.4	82.0	86.4	107.6	135.1	158.3	144.2
Dieldrin	7.8	20.3	38.4	41.7	42.5	28.2	(73.4)	62.3	41.2	47.9	67.3	(136.12)
pp'-DDE	N.D.	N.D.	8.6	18.3	66.5	57.7	77.7	97.9	[21.1]	[51.3]	132.0	96.3
TPrP	N.D.	2.3	2.7	21.4	30.5	42.0	41.4	57.2	70.5	99.6	104.2	105.0
TBP	3.9	12.5	20.4	16.4	33.0	43.2	55.4	52.5	48.5	(191.0)	(784.0)	(687.6)
TCEP	2.3	15.9	18.5	24.7	31.8	47.8	45.5	(141.8)	58.9	74.4	(158.8)	(223.1)
TCPP	1.8	9.9	22.5	22.7	33.5	45.0	75.2	61.4	57.9	106.1	(166.3)	(151.5)
TPhP	1.8	3.6	6.6	11.0	11.1	13.5	18.6	(64.7)	17.0	45.2	40.6	(106.1)
TEHP	N.D.	4.4	6.8	4.6	14.2	25.8	28.2	(1103.7)	49.6	(100.2)	39.9	(1474.1)
α-TBECH	9.0	18.1	N.D.	47.0	56.6	70.5	81.4	88.1	96.9	107.4	128.0	146.7
β-TBECH	16.2	26.7	N.D.	37.7	53.9	73.8	59.6	70.6	81.8	87.5	105.3	127.1
BDE-47	0.6	2.3	2.5	8.6	11.6	13.5	29.3	38.3	40.5	43.4	58.1	78.7
10:2 FTOH	25.0	61.8	47.5	(131.4)	59.4	112.8	122.6	83.0	102.8	138.1	231.7	186.0

N.D. means that the chemical was not detected in PAS; N/A means that the data are unavailable; values in round brackets are values judged to be unreliably high; the values in square brackets are values that are judged to be too low.

Table S5 Estimated passive sampling rates (m^3 d^{-1}) using the linear regression between effective sampling volume calculated based on the uptake amount from the PAS-SIM at different stagnant air layer boundary thickness and deployment length

Chemicals	Estimated *SR*s at Different Air Film Thickness			
	7.5 mm	10.0 mm	15 mm	20 mm
OCPs	0.11	0.10	0.10	0.09
HCBD	0.35	0.31	0.26	0.22
PeCB	0.29	0.27	0.23	0.19
TBA	0.46	0.39	0.30	0.24
α-HCH	0.45	0.39	0.30	0.24
TeCV	0.39	0.35	0.28	0.23
HCB	0.55	0.45	0.34	0.27
DAME	0.49	0.42	0.32	0.26
PCA	0.47	0.40	0.30	0.25
γ-HCH	0.49	0.41	0.31	0.25
δ-HCH	0.67	0.52	0.36	0.28
Heptachlor	0.49	0.39	0.27	0.21
TC	0.61	0.48	0.33	0.26
CC	0.64	0.50	0.35	0.26
TN	0.70	0.54	0.37	0.28
Dieldrin	0.67	0.52	0.36	0.27
pp'-DDE	0.11	0.10	0.10	0.09
OPEs				
TPrP	0.33	0.29	0.24	0.20
TBP	0.52	0.42	0.30	0.24
TCEP	0.45	0.39	0.30	0.24
TCPP	0.31	0.28	0.23	0.19
TPhP	0.66	0.51	0.35	0.26
TEHP	0.49	0.38	0.26	0.20
HFRs				
α-TBECH	0.54	0.44	0.32	0.26
β-TBECH	0.54	0.44	0.32	0.25
BDE-47	0.69	0.53	0.36	0.28
nPFAS				
10:2 FTOH	0.11	0.11	0.10	0.09
Average*	0.53 ± 0.11	0.43 ± 0.07	0.31 ± 0.04	0.25 ± 0.03

* The averages were calculated for all chemicals except the chemicals that were defined as no agreement in Figure S4, namely, PeCB, TBA, HCBD, and 10:2 FTOH.

Table S6 The precursor, product ions and collision energy (CE) for GC-MS/MS detection

Chemicals	Precursor ion	Product ion	CE (eV)
Spiking Standards			
Labeled OPEs			
d_{15}-TEP	167.7	103.0	15
	167.1	83.0	45
d_{21}-TPrP	151.1	102.9	5
	199.2	103.0	5
d_{15}-TPhP	341.1	223.2	35
	341.1	176.0	60
d_{12}-TCEP	261.0	196.1	5
	263.0	131.0	10
$^{13}C_2$-TBEP	201.1	103.0	5
	303.2	103.0	5
d_{15}-TDCPP	394.0	163.9	10
	396.0	163.8	10
d_{27}-TBP	167.1	103.0	5
	231.2	103.0	5
Labeled OCPs			
$^{13}C_6$-PCA	270.9	241.8	15
$^{13}C_6$-PeCB	255.9	220.7	30
$^{13}C_6$-α-HCH	188.8	153.0	15
$^{13}C_6$-HCB	289.9	254.9	20
$^{13}C_{10}$-HEP	276.5	241.9	20
$^{13}C_{10}$-TC	384.9	273.6	25
$^{13}C_{12}$-PPDDE	257.5	187.6	35
$^{13}C_9$-Endo II	250.7	214.6	15
$^{13}C_{12}$-p,p-DDT	405.8	335.9	25
Labeled HFRs			
$^{13}C_{12}$-BDE 28	417.8	257.9	20
	419.8	260.0	20
$^{13}C_{12}$-BDE 47	337.9	148.9	55
	497.7	337.9	25
$^{13}C_{12}$-BDE-99	575.6	415.7	26
	575.6	417.7	26
$^{13}C_{12}$-BDE 139	497.7	228.0	60
	655.7	495.7	40
$^{13}C_{12}$-BDE180	573.7	413.8	45
	575.7	415.8	45
BDE205	641.7	534.5	50
	801.7	641.7	25
$^{13}C_{12}$-BDE209	811.8	651.4	45
	971.4	811.3	32
$^{13}C_6$-PBBz	480.0	319.7	45
	481.8	240.9	60
$^{13}C_6$-HBBz	397.7	316.8	25
	477.6	397.7	30
$^{13}C_6$-EHTBB	428.9	240.9	60
	444.9	321.9	60
$^{13}C_6$-BEHTBP	128.3	62.1	15
	128.3	80.5	5
$^{13}C_6$-BTBPE	362.8	95.1	55
	364.8	283.9	10

$^{13}C_{10}$-anti-DP	277.0	242.0	25
	279.0	244.0	25
$^{13}C_{14}$-DBDPE	491.7	331.8	60
	493.6	333.9	60
$^{13}C_{10}$-Dec-602	277.0	242.0	20
Injection Standards			
TAP	168.8	99.0	5
	238.8	99.1	10
$^{13}C_{12}$-PCB105	335.9	266.0	28
$^{13}C_{12}$-PCB180	405.7	335.9	30
	407.6	373.0	15
$^{13}C_{8}$-Mirex	275.7	240.5	20
Native Standards			
Halogenated methoxybenzene			
DBA	265.5	222.9	30
	263.9	222.9	30
TBA	343.9	300.8	35
	345.6	302.8	35
PCA	264.7	236.8	15
	279.9	264.8	10
TeCV	275.9	260.9	10
	260.9	217.9	20
DAME	275.9	260.9	10
	260.9	217.9	20
Industrial organochlorines			
HCBD	224.8	189.9	20
	222.8	187.8	20
HCCPD	234.6	140.8	35
	236.6	142.8	35
PCNB	236.9	142.9	20
	295.0	236.8	20
PeCB	249.9	214.9	20
	247.7	212.8	20
HCB	283.7	248.8	25
	285.7	250.7	25
TCNB	260.9	202.9	15
	258.9	200.9	15
Metabolic by-products of pesticides			
PCAN	263.0	191.9	25
	265.0	193.9	25
PCTA	295.8	245.8	35
	293.8	243.8	35
Oxchlord	386.7	322.5	10
	388.7	324.5	10
OCPs			
α-HCH	180.8	144.9	15
	182.8	146.8	15
β-HCH	180.8	145.1	15
	182.8	146.9	15
γ-HCH	180.8	145.1	15
	182.8	146.9	15
δ-HCH	180.8	145.1	15
	182.8	146.9	15
pp'-DDE	245.9	176.0	30

	247.9	176.0	35
op'-DDD	234.9	165.0	25
	236.9	165.0	30
o,p-DDE	245.9	176.0	40
	247.9	176.0	40
pp'-DDD	234.9	165.0	25
	236.9	165.2	25
op'-DDT	234.9	165.0	25
	236.9	165.0	25
pp'-DDT	234.9	165.0	25
	236.9	165.0	25
Aldrin	262.7	227.7	25
	264.7	229.7	20
CC	372.7	265.7	25
	374.7	265.8	25
Dieldrin	264.8	229.8	20
	262.7	227.7	20
α-Endo	240.8	206.0	20
	241.0	136.0	25
β-Endo	240.8	206.0	15
	238.8	203.9	20
Endo S	273.6	239.0	15
	271.6	236.9	15
Endrin	278.8	242.8	10
	280.8	244.8	10
HEPT	271.8	236.6	20
	273.6	238.7	20
Hepx	352.7	262.7	20
	354.7	264.8	20
Methoxychlor	227.4	141.0	40
	227.4	169.1	35
Mirex	273.7	238.7	20
	271.7	236.8	20
Photomirex	273.6	239.0	20
	271.9	236.8	20
TC	372.7	265.7	25
	374.7	265.8	25
TN	408.7	299.8	25
	406.7	297.8	25
OPEs			
TEP	155.1	99.0	50
	99.0	80.9	20
TPrP	141.9	98.9	5
	183.1	99.0	5
TBP	99.0	81.0	20
	155.0	99.0	5
TCEP	249.0	187.0	5
	249.0	125.0	10
TCPP	201.0	125.0	5
	201.0	99.0	25
TDCPP	191.0	75.0	10
	380.9	158.9	10
TPhP	326.1	169.2	35
	326.1	214.9	35

TBEP	199.0	101.1	5
	299.0	199.0	5
EHDPP	251.0	77.0	35
	250.0	170.0	5
TEHP	99.0	81.0	25
	113.0	95.0	20
ToTP	368.1	181.2	5
	368.1	165.0	60
TmTP	368.1	165.0	60
	368.1	243.0	35
TpTP	368.1	243.0	35
	368.1	197.3	35
T2IPP	118.0	91.0	35
	118.0	77.0	35
T35DMPP	410.2	193.1	35
	410.2	104.0	35
TDBPP	219.0	99.0	5
	217.9	137.0	5
HFRs			
ATE	329.8	140.8	40
	331.8	142.9	30
α-TBECH	264.9	105.1	10
	266.9	105.0	10
β-TBECH	264.9	105.1	10
	266.9	105.0	10
BATE	329.8	140.8	40
	331.8	142.9	30
PBBz	471.5	311.8	50
	473.5	313.7	50
PBT	406.7	246.9	45
	485.7	406.8	20
PBEB	484.7	405.7	20
	499.7	484.7	20
DPTE	329.8	140.9	50
	331.8	142.9	50
HBB	549.7	470.7	25
	551.8	391.6	50
Dec-602	271.8	236.9	20
	273.6	238.9	20
EHTBB	422.8	313.8	40
	422.8	394.7	25
DEC604	417.8	338.8	15
	419.8	259.9	25
BEHTBP	462.7	378.7	40
	464.7	380.7	40
S-DP	273.6	238.8	25
	271.8	236.9	25
a-DP	271.8	236.9	25
	273.6	238.8	25
DBDPE	484.7	324.7	60
	486.7	326.7	50
BTBPE	356.8	251.9	25
	358.8	251.9	30
BDE 17	245.9	139.0	35

	405.8	246.0	20
BDE 28	245.9	139.0	35
	405.8	245.9	20
BDE 47	325.9	217.0	30
	485.7	325.9	20
BDE 49	325.9	217.0	30
	485.7	325.9	20
BDE 66	325.9	217.0	30
	485.7	325.9	20
BDE 71	325.9	217.0	30
	485.7	325.9	20
BDE 85	403.8	296.8	35
	565.7	405.9	25
BDE 99	403.8	296.8	35
	565.7	405.9	25
BDE 100	403.8	296.8	35
	565.7	405.9	25
BDE 138	483.7	323.8	50
	643.7	483.4	25
BDE 153	483.7	323.8	50
	643.7	483.4	25
BDE 154	483.7	323.8	50
	643.7	483.4	25
BDE 183	561.7	454.5	50
	721.7	561.7	25
BDE 190	561.7	454.5	50
	721.7	561.7	25
BDE 209	799.7	639.8	50
	959.4	799.3	32

Table S7 The target and qualifier ions for GC-MS detection

Chemicals	Target Ion	Qualifier Ion
Spiking Standards		
Labeled nPFASs		
$^{13}C_2$-6:2 FTOH	369	331
$^{13}C_2$-8:2 FTOH	469	497
$^{13}C_2$-10:2 FTOH	569	531
$^{13}C_8$-FOSA-I	508	
d_7-N-MeFOSE-M	547	565
d_9-N-EtFOSE-M	563	581
d_5-N-EtFOSA-M	533	
d_3-N-MeFOSA-M	517	
Native nPFASs		
6:2 FTA	433	461
6:2 FTOH	365	327
8:2 FTA	519	547
8:2 FTOH	465	427
NNMe2FOSA	528	
10:2 FTA	619	647
10:2 FTOH	565	527
EtFOSA	528	
MeFBSA	314	
MeFOSA	514	
MeFOSE	540	558
EtFOSE	554	572
FOSA	500	
FHxSA	400	
FBSA	300	

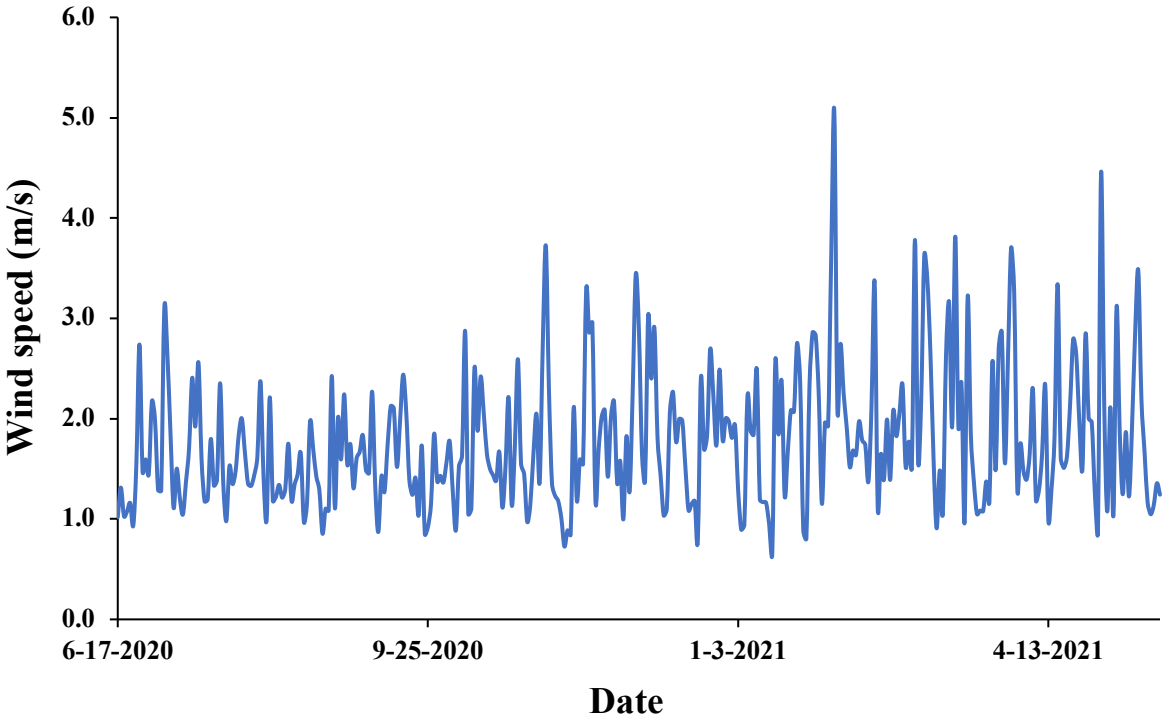

Figure S1. Wind speed recorded by the weather station located on the top of Science Wing building at the University of Toronto Scarborough during the whole sampling period

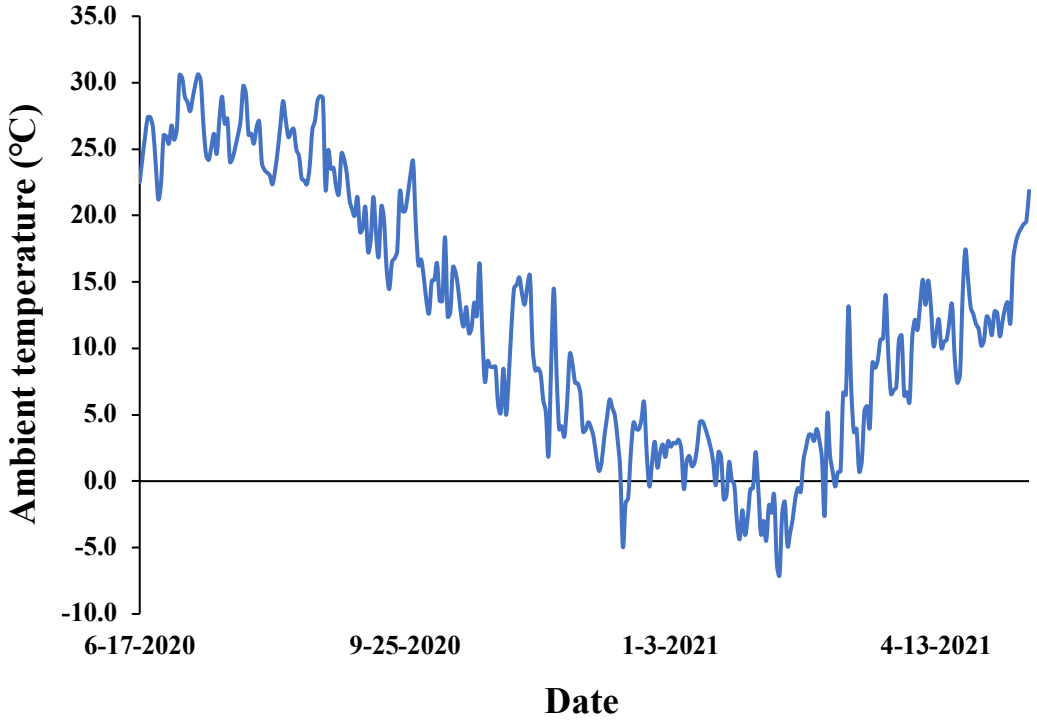

Figure S2. Ambient temperature recorded by us using hourly resolution thermometers (ibuttons) during the whole sampling period

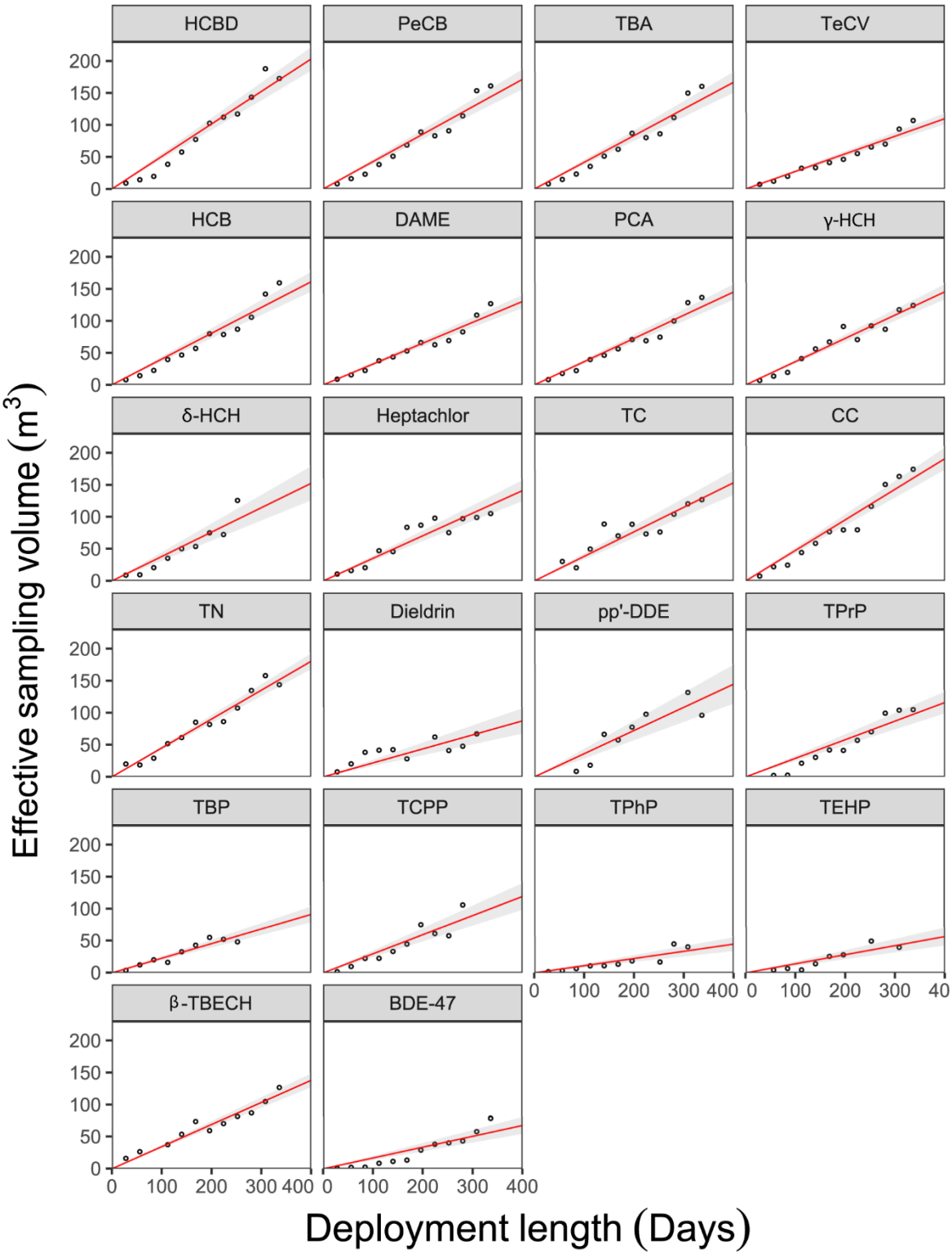

Figure S3. The increase of the effective sampling volume of 22 chemicals throughout the 48-week deployment period. The black markers indicate the field blank-corrected measured values, and the red lines indicate linear regressions forced through the origin. The shaded areas represent the 95% intervals of the linear regressions.

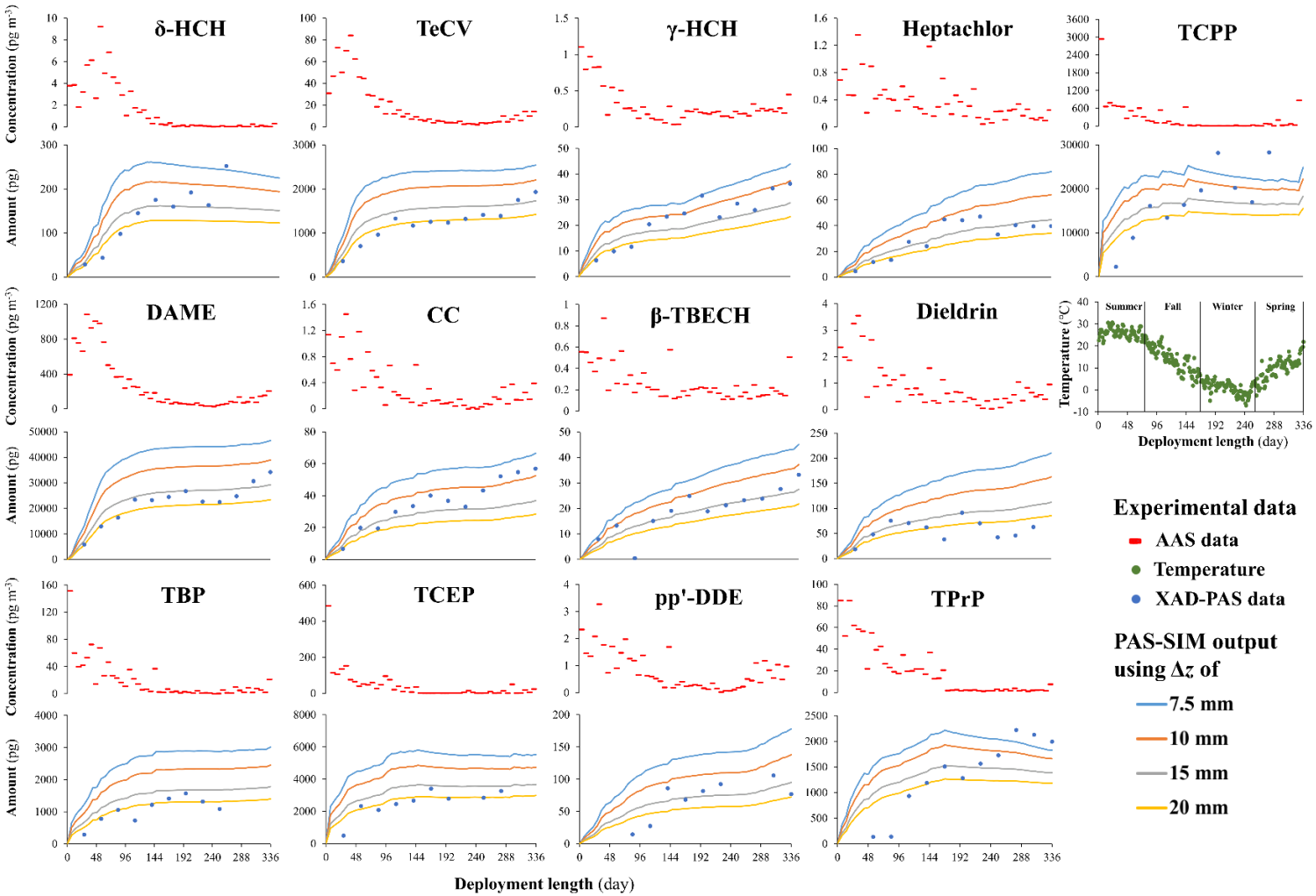

Figure S4: PAS-SIM results for remaining thirteen representative chemicals showing good agreement with measured uptake curves. The red lines in the upper portion of each panel display air concentrations (pg m^{-3}) measured by active air sampling, the blue, orange, prey, and yellow lines are the PAS-SIM model outputs (pg per sampler) under different assumptions regarding the thickness of the stagnant air boundary layer Δz of 7.5, 10, 15, and 20 mm, and the dark blue dots are the experimental data of XAD-PAS obtained from the calibration study (pg per sample). Green markers in the upper right panel display ambient temperature (°C).

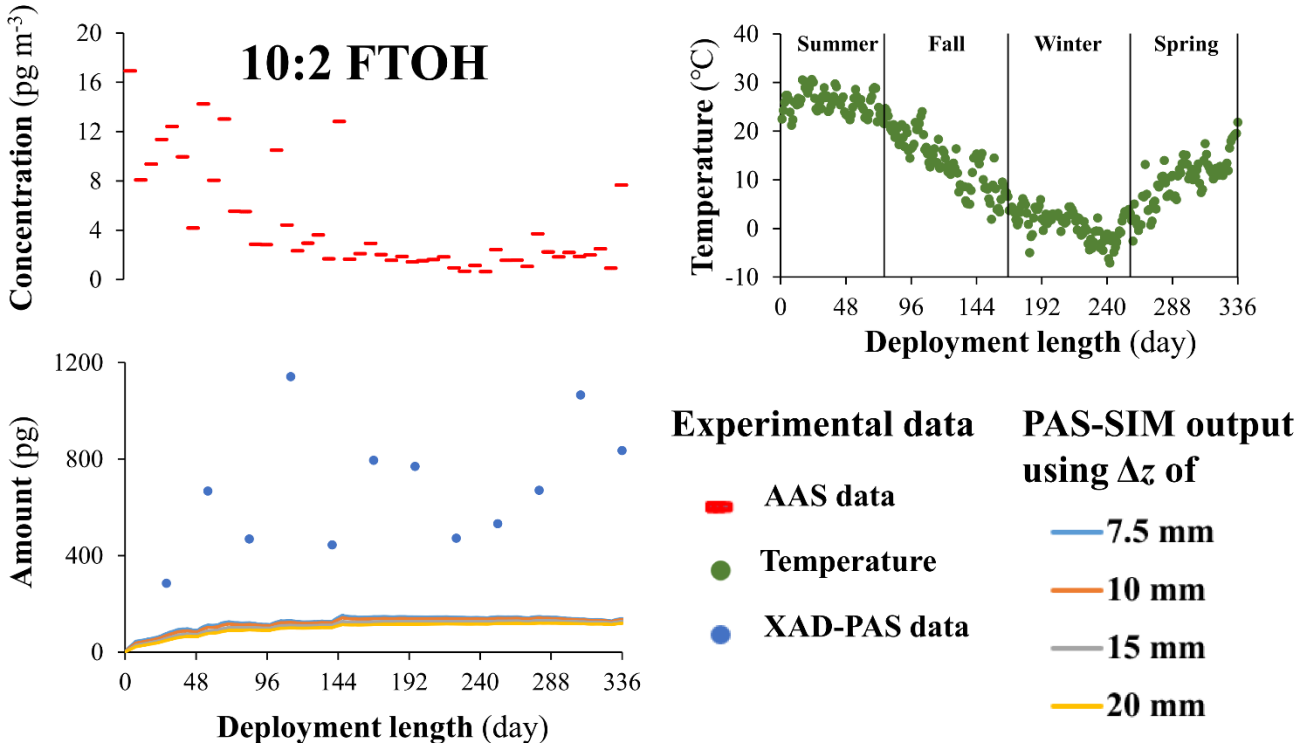

Figure S5: PAS-SIM simulation results for 10:2 FTOH showing consistent underprediction relative to the measured uptake curves. The red lines in the upper portion display air concentrations (pg m^{-3}) measured by active air sampling, the blue, orange, prey, and yellow lines are the PAS-SIM model outputs (pg per sampler) under different assumptions regarding the thickness of the stagnant air boundary layer Δz of 7.5, 10, 15, and 20 mm, and the dark blue dots are the experimental data of XAD-PAS obtained from the calibration study (pg per sample). Green markers in the upper right panel display ambient temperature (°C).

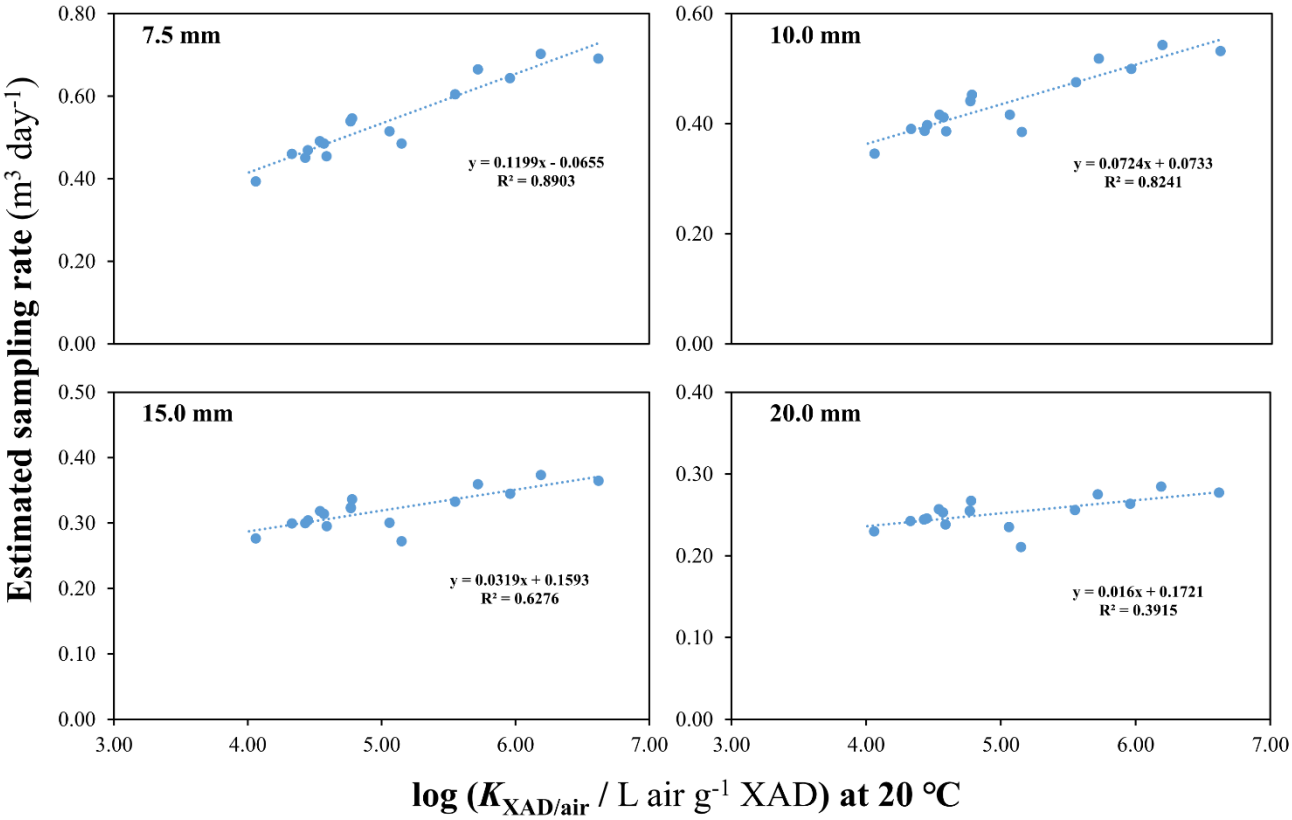

Figure S6: Relationship between the sampling rates estimated from PAS-SIM output, at different stagnant air layer boundary thicknesses, and the logarithm of partitioning constants between XAD and air at 20 °C for chemicals of which the estimated uptake curves had good agreements with measurements. The number on each panel is the assumed boundary thickness of the stagnant air layer.

References

(1) Gawor, A.; Shunthirasingham, C.; Hayward, S. J.; Lei, Y. D.; Gouin, T.; Mmereki, B. T.; Masamba, W.; Ruepert, C.; Castillo, L. E.; Shoeib, M.; et al. Neutral Polyfluoroalkyl Substances in the Global Atmosphere. *Environ. Sci. Process. Impacts* **2014**, *16* (3), 404–413.